Landscape structures regulate the contrasting response of recession along rainfall amounts

Jun-Yi Lee[1,2], Ci-Jian Yang[2,3], Tsung-Ren Peng[1], Tsung-Yu Lee[4], Jr-Chuan Huang[2]

[1]Department of Soil and Environmental Sciences, National Chung Hsing University, Taichung 402202, Taiwan
[2]Department of Geography, National Taiwan University, Taipei 106319, Taiwan
[3]German Research Centre for Geosciences (GFZ), Telegrafenberg, Potsdam 14473, Germany.
[4]Department of Geography, National Taiwan Normal University, Taipei 106209, Taiwan

Correspondence to: Jr-Chuan Huang(riverhuang@ntu.edu.tw)

Abstract. Streamflow recession ~~discloses~~reflects hydrological functioning, runoff dynamics, and storage status within catchments. ~~Understanding recession response to landscape~~Landscape structures and rainstorms ~~can be a guidance~~are regarded and hypothesized as drivers of recession response, which is an important consideration for ~~assessing streamflow change~~regional water resources management, particularly under climate change. Yet, the documented recession response ~~direction of recession~~ is inconsistent and diverse. This study tested how landscape structures and ~~rainstorms~~rainstorm characteristics regulate the recession response~~ direction. We derived a~~. A total of 291 pairs of recession parameters—the recession coefficient, *a*, and nonlinearity, *b*, from the power-law recession model ($-dQ/dt = aQ^b$)~~—~~over ~~all~~ 19 subtropical ~~catchments~~small mountainous rivers with a broad rainfall spectrum~~. Results~~ were derived using the decorrelation process. The results showed that ~~the recession coefficient increases with the drainage density and~~*a* and *b* respectively increase and decrease with *L*/*G* (the ratio of flow-path length to gradient), particularly in small catchments~~, indicating that catchments with the dense network more short-and-gentle hillslopes would result in high values of *a*. Apart from landscape structure, the *a* decreases~~. Additionally, corroborating previous studies, *a* decreased significantly with rainfall amount~~ particularly in low L/G catchments. Probably because rainstorm facilitates connectivity in the saturated zones, which might conjoin more water from slow reservoirs and thus water drains slowly. Additionally, ~~. However, nonlinearity increases with rainfall amount in larger catchments but ~~decreases~~decreased in small catchments. ~~The swing of~~This contrasting response~~ direction~~, which ~~lies in the predominance between~~was contingent upon drainage area and *L*/*G*, leads to considerable bias and needs further clarification, particularly for use in assessing regional recession ~~assessment~~in ungauged catchments under climate ~~changes. Incorrect response direction from landscape structure would lead to considerable bias inference.~~change.

1 Introduction

Streamflow recession, the falling segment of a hydrograph, ~~reflects a~~ represents the rainfall-runoff process and ~~interaction~~interactions among different runoffs and aquifers during a rainstorm. Therefore, recession~~, associated~~ and its associations with runoff paths within the landscape and aquifers, is particularly critical for baseflow estimation (Palmroth et al., 2010). ~~Previous studies analyzed aggregated long-term data to retrieve recession parameters (e.g., Brutsaert and Nieber, 1977), but parameters from individual events can elucidate the recession characteristics of catchments (Jachens et al., 2020) and shed insight into the sensitivity of catchments to rainstorms, which is informative for water resource management. Therefore, recent studies have shifted to investigate recessions from individual events (Biswal and Nagesh Kumar, 2014; Jachens et al., 2020).~~ A power-law relationship, $-dQ/dt = \hat{a}Q^b$, between streamflow declines ~~(~~and streamflow rate Q ~~recesses with a timestep t) with streamflow rates ($-dQ/dt = \hat{a}Q^b$) can~~ is widely used to describe ~~the~~ recession ~~characteristics~~ at the catchment scale (e.g. Brutsaert and Nieber, 1977). ~~Parameter~~The recession coefficient, $\hat{a}$, approximates ~~to~~ the recession rate but is ~~influenced by~~ tangled with the unit of ~~flow~~streamflow and b (see section 2.2.2), ~~and parameter b~~ which represents the nonlinearity of storage~~. Recession parameters are often linked to the aquifer geometries, landscape,~~ and ~~spatial heterogeneity.~~is the slope of the regression line of dQ/dt vs Q. Since ~~the aquifer~~aquifers in various landscape units (e.g., ~~hillslope~~hillslopes, riparian~~, stream) exhibits~~ areas, streams, etc.) exhibit different hydraulic properties~~ and~~, landscape structure~~, which presents the geometry of catchments and aggregates catchment hydraulic properties,~~ apparently ~~reflects various~~affects the streamflow recession parameters. In ~~theory~~general, parameter $\hat{a}$ has a positive correlation with drainage density (total stream length/drainage area) and aquifer ~~slopes~~slope but a negative correlation with aquifer ~~depths~~depth, aquifer heterogeneity~~ (of conductivity)~~, and inter-hillslope heterogeneity (e.g., Brutsaert and Nieber, 1977; Rupp and Selker, 2006~~) and inter-hillslope heterogeneity (of celerity) (~~; Harman et al., 2009). Parameter b increases with the number of streams (Biswal and Marani, 2010), ~~the~~aquifer heterogeneity ~~of the aquifer~~ (Rupp and Selker, 2006~~)~~), and ~~the~~ inter-hillslope heterogeneity (Harman et al., 2009~~), yet decrease~~) and decreases with the total stream length (Biswal and Marani, 2010).

Theoretical works ~~also~~ have ~~illustrated~~shown that the ~~temporal dependence of~~streamflow recession parameters are dependent on ~~the groundwater table, recharge,~~landscape structure (and thus aquifer conditions) and ~~storage. From the perspective of temporal variability,~~rainstorms. Rupp and Selker (2006) demonstrated that parameter $\hat{a}$ is negatively correlated ~~to~~with the initial groundwater table (h_0) under unsaturated conditions~~ and renders~~, while it has a slightly positive correlation under saturated conditions ($h_0 \geq B\tan\phi$, where B is aquifer length and ϕ is ~~ϕ~~the aquifer angle~~, Rupp and Selker, 2006). A large recharge rate also reduces parameter $\hat{a}$, particularly in homogenous catchments (Harman et al.,~~). Harman et al. (2009~~). On the other hand~~) used spatial heterogeneity theory to show that a large recharge rate reduces parameter $\hat{a}$, while drainage network theory suggests that parameter $\hat{a}$ is negatively correlated with the streamflow rate (Biswal and Nagesh Kumar, 2014). For parameter b, hydraulic theories indicate that b decreases from 3.0 to 1.5 during the transition from early to late recession~~,~~ as the ~~groundwater is vertically sourced from different hydraulic properties~~influence of the upstream boundary condition becomes a factor when the aquifer drains in wet conditions (e.g., Rupp and Selker, 2006). ~~The spatial~~Spatial heterogeneity theory demonstrates that b only slightly increases with ~~the~~a wet antecedent condition (Harman et al., 2009). However, ~~the~~ drainage network theory indicates that b increases~~/decreases~~ with storage while ~~reaches in~~the downstream ~~are contributed by~~receives more~~/fewer~~ subsurface ~~storages~~flow contribution but decreases with storage as the downstream receives less (Biswal and Nagesh Kumar, 2013). The ~~various~~inconsistent responses in $\hat{a}$ and b among theories ~~implying the control of~~ indicate a complicated interaction between landscape structure and ~~rainfall amount on~~rainstorms during recession, implying that the recession mechanics in different regions ~~should be improved.~~ need more exploration.

~~The compilation of pervious~~Tables 1 and S1 respectively summarize and compile previous empirical recession ~~works (summarized in Table 1 and S1) demonstrated that most~~ studies ~~elucidated the recession parameters at long-term scale, and the relationships between recession parameters against landscape, landcover, and soil were inconsistent. For example, empirical recession parameters have inconsistent~~ . There are two main takeaways: 1) The responses of $\hat{a}$ and b to ~~several physiographic variables (drainage area, drainage density, water bodies coverage,~~landscape features and ~~surface saturated conductivity), implying that different~~ structure have been inconsistent. Such inconsistent results might be landscape ~~regimes may have distinct~~ dependent (e.g. different regional conditions). 2) These inconsistent recession responses~~. Additionally, most inter-event studies just analyzed the single parameter ($\hat{a}$) that decreases with the catchment wetness, which ignores~~ might be due to different treatments (e.g. segment extraction, starting point, fitting techniques, etc.). Most previous studies aggregated long-term data (point-cloud) to retrieve representative recession parameters (the centrality of recession), while some recent studies retrieved parameters from individual events to elucidate the temporal variability of ~~b. Only~~ recession. Fewer studies simultaneously addressed recession responses to landscape structure and distinct rainstorm events, which are likely dependent on $\hat{a}$ and b in the power law. For example, Biswal and Nagesh Kumar (2013) found ~~the different~~ that the structure of drainage networks might result in contrasting directions ~~of b~~in the response of b to peak flow~~, but which landscape variables would control the direction is still unclear. This compilation indicated that rare studies focused on the subtropical region and the variability of recession parameters at event scale.~~.

~~This study investigated the recession parameters along with different magnitude of rainstorms (e.g. typhoons) on steep landscape in hope to identify the interactive role of rainfall and physiographic variables in recession. Specifically, we~~ Everything considered, the theory behind recession is still developing, and it is clear that we need a better understanding of how landscape structure and rainstorm characteristics affect streamflow recession, especially with the necessity of regional recession assessments under climate change. Thus, this study derived the recession coefficient and nonlinearity in 19 mountainous catchments ~~(drainage area varies between 77–2,089 km^2)~~ across Taiwan with multiyear records of hourly streamflow (291 events in total). ~~Due to frequent tropical cyclones (alias:~~These catchments, with drainage areas of 77–2,089 km^2, are characterized by steep, fractured, forested mountains and periodic typhoon~~) and mountainous landscapes~~ invasions. As a result of these characteristics, Taiwan's rivers ~~lead to~~have short water ~~travel~~residence time and ~~limit~~limited water retention capacity ~~in catchments~~ (Lee et al., ~~2020). Most typhoon rainwater falls in summer and elevates water level dramatically but diminishes quickly within 2-3 days (Huang et al., 2012). Here, the following~~2020). We addressed three research questions ~~are addressed~~: (1) What are the recession characteristics of typhoon events in ~~subtropical~~small mountainous catchments? (2) How do rainfall and landscape variables affect recession parameters in different ~~landscape regimes?~~regions? (3) In what way do landscape variables regulate the response of nonlinearity to rainfall? ~~We documented~~In this study, we document the spatial patterns of recession parameters in Taiwan (Sect. 3) and then discussed how ~~the~~ recession behaviors change in different landscape settings (Sect. ~~4). Finally, we proposed a hypothesis: landscape structure could swing recession responses to~~

rainstorms. Understanding the recession behaviors after typhoons are vital to water resource management, particularly when global warming likely increases the frequency and magnitude of flood and drought (Shiu et al., 2012; Huang et al., 2014).4).

2 Material and methods

2.1 Study area

Taiwan is a mountainous island geographically located at the juncture between the Eurasian and Philippine tectonic plates and climatologically located atin the corridor of typhoons. TheAn active mountain belt with frequent typhoons shapes a steep and fractured landscapeslandscape with verdant forests. The mean annual rainfall is about 2,510 mm, and approx. 40% of annual rainfall is brought by typhoons inwithin a few days. The lowest mean annual temperature is approx. 4°C in montane regions and 22°C in plain regions. In this mountainous island, the upliftingthe coastal plains. The mountains of Taiwan reach an elevation (0 of 4,000 m) within a short horizontal distance (~75 km) showsfrom the coast, creating a steep terrain (Huang et al., 2016). Specifically, the drainage area of most catchments is smaller than ~500 km^2, and stream lengths are less than ~55 km, indicating a short water travel time.. The basic catchment descriptions of, including landscape variables could refer to, can be found in Table S2. Land cover inventories from the Taiwan Ministry of the Interior (www.moi.gov.tw) were reclassified from the original 13 categories into three major categories;, namely, water (C_W), forest (C_F), agriculture (C_A), and others for each catchment.. The landscape metric described by the landscape variables werewas retrieved from the digital elevation model (DEM) with 20m resolution and referred to Table S2. The specific definitions of landscape variables are below: A is the drainage area [L^2]; DD is the drainage density [L/L^2]], defined as the ratio of total stream length to drainage area; S_m is the gradient of mainstreamthe main stem [-]; HI is the hypsometric integral [-]; ELO is the basin elongation [-][-], defined as the ratio of the diameter of the circle (with the same area withas the basin) to basin length. Notably, theThe flow- path is defined as the hillslope grid point following the surface flow direction toward the channel. Flow-path length (L) is the length of this path, and flow-path height (H) is the height difference along this path., and G is the flow-path gradient [-]. These flow-path metrics and the L/G ratio, as proxies for the interaction between landscape and climate (Seybold et al., 2017), are often used in transit timethe studies of water residence time (e.g., McGuire et al., 2005), helping to describe how landscape control on streamflow recession.)

Streamflow in this steep mountainous island usually descends quickly after a considerable surge by a typhoon invasion. Thus, hourly streamflow records are required to describe the entire streamflow recession since it only lasts a few days after the peak. This study selectedcollected hourly streamflow records during 1986-2014 from the Taiwan Water Resource Agency (www.wra.gov.tw) and Tai-Power Company (www.taipower.com.tw). Only the catchments without large water division infrastructures in the upstream area and thewith total rainfall largergreater than 30 mm were used to preventavoid human manipulation on-manipulated streamflow and guarantee the discharge rise.data. Based on thethese criteria, nineteen catchments and 291 events were filteredincluded for further recession analysis. Commensurate with the hourly streamflow, the hourly rainfall dataset from the Taiwan Central Weather Bureau (www.cwb.gov.tw) was introduced to collected, and the Thiessen weighted method forwas used to estimate areal rainfall estimation toin the corresponding catchments. The rainfall period was defined as the elapseelapsed time from 6 hrh before the rising flow to the peak flow. Collectively, a hydroclimate metricHydroclimate metrics of rainstorm and streamflow presented, including total event rainfall, duration, average and maximum rainfall intensity, total streamflow, peak flow, and antecedent flow is shown in , were extracted from these datasets (Table S3.).

2.2 Recession analysis

As most analyses of hydrological processes do, the water balance equation is primarily described as Eq. (1):

$\frac{dS}{dt} = P - E - Q$ The storage-outflow relationship is typically described by a power law if treating the catchment as a black box. The representative storage is, in fact, composed of many aquifers and thus exhibits a non-linear relationship:

$$Q = mS^n \qquad (1)$$

where S is the storage volume within a catchment (in units of volume [L^3] or depth [L]), and P, E, and Q areis the ratesrate of precipitation [L], evapotranspiration [L], and stream discharge [streamflow ([L^3/T] or [L/T], respectively. For solving the unknown storage, which cannot be measured directly, all terms should be identified. The formula $Q = mS^n$ with constant]), and m and n are constants (Vogel and Kroll, 1992), which follows Dupuit-Boussinesq equation, can be used). Since S is difficult to derivedirectly measure, the relationship between storage and stream discharge. In this regard, S can be replaced by Q to infer the storage changes. During the recession period, P and E are relatively small compared to Q, and then the following equation is the rate of streamflow decline and streamflow could be derived to represent the recession behaviors within a catchment.behavior (Brutsaert and Nieber, 1977) in Eq. (2).

$$-\frac{dQ}{dt} = nm^{\frac{1}{n}}Q^{\frac{2n-1}{n}} = \hat{a}Q^b \qquad (2)$$

where $\hat{a}$ is the recession rate and b are constants derived from the Q-S relation. In this study,represents the stream discharge has been normalized by drainage area,nonlinearity of storage, which is also the slope of the regression line in the plot of dQ/dt vs Q (the recession plot). Both parameters can be estimated via different assumptions and fitting techniques. Notably, since nonlinearity is dimensionless, $\hat{a}$ is inherently strongly dependent on the unit of Q, $\hat{a}$ and b is [mm/h], [h^{-1}(mm/h)$^{1-b}$] and [-], respectively. This power-law form between $-dQ/dt$ and Q indicates that the rate of streamflow decline is highly relevant to Q during the recession and has been widely plotted as “recession plot” (Kirchner, 2009). This plot via fitting (see details in section 2.2.2). Although the recession plot enables the analysis of streamflow recessions aggregatedly or event-independently recession and facilitates the derivation of the storage–outflow relationships relationship (Stölzle et al., 2013). Although the power-law formula and recession plot are widely used for describing the recession behavior, the retrieval procedures of recession), the methods of recession segment extraction andmanipulate parameter estimation are diverse due to different practical operations.. For example, Stölzle et al. (2013) compared three extraction methods of recession segment in conjunction with their corresponding parameter estimations~~ and all possible combinations.~~. They found that recession characteristics, like recession time (1/~~a)~~$\hat{a}$), varied over 1–2 orders of magnitude, yet ~~exponent b differed~~nonlinearity, b, varied rather narrowly. Their results suggested that the recession characteristics derived ~~with~~from different procedures have only limited comparability ~~and highlight the distinctiveness of individual procedures due to different purposes and philosophies.~~. Further, Dralle et al. (2017) ~~also agreed with the above statement but they~~ found that the relationship between $\hat{a}$ and antecedent wetness ~~were~~was sensitive to the ~~length~~number of data~~.~~ points and thus the extraction method. Despite the ~~differences~~estimated parameters being inconsistent among the procedures, applying the same procedure ~~to a regional extent~~is still ~~captures the recession characteristics. The following subsections present the procedures used for extraction and parameter estimation.~~ a feasible way to capture the recession responses in a region.

2.2.1 Recession segment extraction

In the extraction procedure, two concerns should be addressed: (1) distinguishing between the early and late recession ~~stage~~stages, and (2) ~~elimination of the~~eliminating any unexpectedly positive increases in the recession. The early~~-~~ stage (containing ~~preceding~~ pre-storm and surface flow) and the late stage of recession (~~only~~ dominated only by base flow) are indistinguishable and usually determined subjectively~~ based on different purposes.~~. Some studies have empirically excluded the early-stage recession ~~from eliminating~~ to eliminate the influence of quick flow (e.g., Brutsaert, 2008; Vogel and Kroll, 1992). ~~Some other studies~~Others used a threshold for the minimum length ~~in~~of extraction procedures, which ranged from 2~~-~~ to 10~~-~~ days (e.g., Mendoza et al., 2003; Vogel and Kroll, 1992). For eliminating ~~unexpectedly~~unexpected positive increases ~~in~~during recession, several approaches have been proposed as well, for example, smoothing the hydrograph (Vogel and Kroll, 1992), discarding the segment ~~directly~~entirely (Brutsaert, 2008; Kirchner, 2009), and breaking-and-rejoining the recession segments (Millares et al., 2009). Each strategy has its advantages and disadvantages; smoothing the hydrograph ~~could~~may not completely erase the ~~bulge~~bulges caused by precipitation~~;~~ and discarding the segment ~~would lose part~~loses parts of recession events. Although breaking-and-rejoining the recession, too, disturbs the original streamflow records, the method which maintains ~~a better integral of a~~the more complete recession event is preferable here.

~~The specific procedure of~~ For the recession segment ~~used in this study was described below. First~~extraction, first, the recession evolution caused by ~~typhoons is our~~rainstorms was a main concern, and thus we selected the whole recession segment from the peak flow of ~~the~~all individual rainstorm. The whole recession segment represents the interactive mixing of quick and base flow~~ interactively. Later~~. Second, we screened and broke down the hydrograph ~~as an~~where abrupt ~~bulge~~bulges emerged, erased ~~the~~ positive streamflow increases, and concatenated the remaining segments. This elimination procedure ~~is~~produces a curve quite similar to the master recession curve on a long-term scale (Millares et al., 2009). Third, data points corresponding to extremely low streamflow (Q < 0.1 mm h^{-1}) or recession ($-dQ/dt$ < 0.01 mm h^{-2}~~)~~), being likely affected by the limits of streamflow measurement, were excluded~~, due to the undetectable change in recession~~. Forth, rainfall events with an unreasonable ratio of total flow to total rainfall (Q/P > 1.1 or Q/P < 0.1) were also excluded~~.~~ to guarantee the data quality. Ultimately, a total of 298 rainstorms were selected for further parameter estimation.

2.2.2 Parameter fitting

~~Generally, the~~In recession ~~plot (-*dQ*/*dt* vs *Q*) is widely used for estimation of recession parameters. But~~analysis, several fitting methods have been proposed~~ due to different philosophies in the literature.~~. One is to fit with the lower envelope of the point-cloud (Brutsaert and Nieber, 1977~~) since the evapotranspiration effect in a~~). Evapotranspiration affects recession~~ would lead,~~ leading to ~~a~~ higher ~~value~~values of -*dQ*/*dt*~~. Taking~~, and taking the lower envelope can prevent ~~the evapotranspiration~~this effect. Another~~ one~~ is to fit with the entire point-cloud (Brutsaert, 2005; Vogel and Kroll, 1992) as subsoil heterogeneity may overshadow the evapotranspiration effect in larger or steeper catchments (Brutsaert, 2005). ~~The other~~Yet another is to fit with the binned means weighted by the square of the standard error of each binned mean (Kirchner, 2009) because the lower values of -*dQ*/*dt* could be affected by the measurement errors in the streamflow ~~observation~~observations. Recently, a virtual experiment study (Jachens et al., 2020) suggested ~~to fit~~fitting with individual recession segments ~~in order~~ to ~~capture~~explore the recession ~~characteristics and offer an opportunity for exploring the impacts of rainstorm properties. Because a group of data clouds (aggregated dataset) might result in underestimation of nonlinearity (~~responses to individual rainstorms~~Jachens et al., 2020). We, therefore, used each recession segment and fitted it with the power-law recession individually~~.

The ~~specific~~ parameter estimation ~~for~~from the retrieved recession ~~segment~~segments was described below. Firstly, we corrected low-flow ~~record correction: the~~ records: The same low ~~flows~~flow levels appear frequently in late recession due to the detection limit of instruments~~ and result~~, resulting in a series of zero ~~value of~~ -*dQ*/*dt* ~~which affects~~values that affect parameter estimation, particularly ~~in~~for *b*. ~~We~~To reduce this bias, we applied the exponential time step method (Roques et al., 2017) ~~here to reduce the bias,~~ in which the time step of the moving window for calculating -*dQ*/*dt* exponentially increases along the recession. ~~The~~This extended sampling period ~~could~~helps avoid the occurrence of zero -*dQ*/*dt* values ~~of -*dQ*/*dt*.~~(Roques et al., 2017). Secondly, we used the decorrelation method: ~~another~~Another important concern ~~of~~in recession parameter estimation ~~in recession~~ is the dependence between ~~a~~$\hat{a}$ and *b*, which blurs the interpretation of parameters~~. Therefore, we applied~~ (Dralle et al., 2015). The decorrelation method ~~which~~ assumes that the observed flow, *Q*, consists of a scale-free flow $\hat{Q}$ and a constant *k* ($Q = k\hat{Q}$). Thus, the power law formula can be rewritten as $-dQ/dt = ak^{b-1}\hat{Q}^b$, where *a* is the scale-free recession coefficient [h^{-1}]. For correcting $\hat{a}$ to *a*, the observed flow *Q* was divided by a constant Q_0 (which is ideally equal to $1/k$, see detail in Dralle et al., 2015~~). After~~):

$$Q_0 = \exp\left(-\frac{\sum_{i=1}^{N}(b_i - \bar{b})(\log(\hat{a}_i) - \overline{\log(\hat{a}_i)})}{\sum_{i=1}^{N}(b_i - \bar{b})^2}\right) \quad (3)$$

where $\bar{b}$ and $\overline{log(\hat{a})}$ is the means of the fitted parameters *b* $\{b_1, b_2, \ldots, b_N\}$and $\log(\hat{a})$ $\{\log(\hat{a}_1), \log(\hat{a}_2), \ldots, \log(\hat{a}_N)\}$, respectively, across *N* rainfall events in a given catchment. Although the decorrelation method can reduce the unit effect and dependency on *b*, Biswal (2021) argued that the dependency of $\hat{a}$ and *b* can't be fully decoupled, and retrieving parameters from the power law and fixing *b* is preferable. Obviously, decoupling the dependency of $\hat{a}$ and *b* in recession is unsolved and challenging and necessitates further study. Nevertheless, after the decorrelation process, the number of catchments with a high correlation between *a* and *b* (R^2 > 0.1) decreased from 9 to 2~~.~~, apparently mitigating the unit-effect and dependency of *b*. Finally, events with low goodness of fit (R^2 < 0.5) were discarded. ~~Ultimately, each watershed had~~As a result, 291 events and all watersheds, with 5 to 26 events ~~(total is 291, see~~ each (Table S3~~) selected~~), were included for exploring the landscape and rainstorm effects~~, of which events were~~. Each individual storm event may not necessarily ~~the same rainstorm~~occur in all catchments.

3. Results

3.1. Recession parameters from individual and point-cloud ~~fit~~fits

~~After proceeding with the mentioned analysis onto this dataset, we demonstrated the~~The streamflow recession plots of catchments W9, W5, and W8, as examples, are illustrated in Fig. 2. The three catchments have distinct differences in landscape, particularly in drainage area (*A*) and ~~*L/G* (~~the ratio of ~~median~~ flow-path length to ~~median flow-path~~ gradient ~~to stream), see Table S2.~~(*L*/*G*). Catchment W9 has a larger *A* and lower *L*/*G*, W5 has a ~~lower~~smaller *A* and lower *L*/*G*, and W8 has a smaller *A*~~,~~ but higher L/G~~. In~~, see Table S2 for catchment details. Median *b* values, in descending order, ~~the ranking of median recession *b* is catchment W9 (~~were 2.34~~), W5 (~~ in catchment W9, 1.96~~),~~ in W5, and ~~W8 (~~1.63~~).~~ in W8. The point-cloud-derived *b* ~~are~~values were 1.45 (W9), 1.37 (W5), and 0.88 (W8), showing ~~all~~that point-cloud-derived *b* values are smaller than median~~ ones~~-derived values (Fig. 2c). Notably, the nonlinearity decreases with ~~the~~ storm magnitude in W5 and W8~~, yet, the nonlinearity~~ but increases with ~~the~~ storm magnitude in W9 (Fig. 2b and 2c). ~~The opposite responses of W9 and W5/W8 to storm magnitude coincide with the~~This contrasting response coincided with a difference ~~of~~in drainage area~~.~~ and was relatively consistent across all the catchments. This apparent association ~~will be~~is explored further in the Discussion section.

~~Further, the~~The frequency distributions of the fitted recession ~~coefficient~~coefficients and ~~nonlinearity of the total catchment~~ nonlinearities from all catchments and event records are shown in Figure 3a-b. Coefficient~~,~~ *a*~~, ranges~~ ranged from 0.003 to 0.273 hr^{-1} with a mean ~~=~~of 0.059 hr^{-1} and median ~~=~~of 0.047 hr^{-1}. The large difference between the median and mean ~~shows~~reflects a right-skewed distribution. Nonlinearity, *b*, ~~ranges~~ranged from 0.90 to 4.39 with a mean ~~=~~of 1.76 and median ~~=~~of 1.69. The small difference between the median and mean ~~presents an asymmetric~~suggests a relatively symmetric distribution~~ of nonlinearity~~. Spatial patterns of recession coefficient and nonlinearity are illustrated in Fig. 3c-d. Generally, larger recession coefficients ~~are located~~were seen in the southwestern plain ~~(Fig. 3c). Those plain~~ catchments ~~also~~(Fig. 3c), which have higher *L*/*G* values. Apart from this, no other distinct pattern can be found in other, more mountainous catchments. Conversely, the plot of recession nonlinearity presents a vague pattern (Fig. 3d), and no simple relationship could be found.

The recession parameters derived from individual segments and aggregated point-cloud data are illustrated in Fig. 4. The ~~individual segment parameters which demonstrate the~~ variations of recession responses ~~to each event present the holistic variation, whereas the point-cloud parameters that~~ from individual segments fluctuated greatly among catchments. For parameter *a*, point-cloud-derived values, which aggregate all recession segments in ~~specific~~a catchment~~,~~ are ~~generally~~much larger ~~for~~than the ~~coefficient and smaller for the nonlinearity~~coefficients from individual segments. Notably, when the drainage area is larger than 800 km^2 (W19~~), the coefficients from aggregated point-cloud get similar to the~~ and larger), the point-cloud-derived coefficients become similar to the third quantile of the distribution of individual segments. For nonlinearity, the values derived from the point-cloud are consistently close to the lower limit of the distribution of the individual segment-derived values and the median ~~of the individual segment. The coefficients are close to the upper limit from the aggregated point-cloud for small catchments, compared to W19. Besides, the deviations of aggregated point-cloud coefficients are distinctly larger in the small catchments. The median and~~ and interquartile range of nonlinearity derived from individual segments are irrelative ~~to~~of drainage area~~, and the values from the aggregated point-cloud are consistently lower than that from individual segments. Distinct~~. These distinct differences between coefficients and nonlinearities from the two fitting methods ~~present the manipulation of fitting method, which results in the difficulty in~~make comparison and ~~inference.~~interpretation difficult. The details of the recession characteristics for each catchment can be ~~referred to~~found in Table S4.

3.2 ~~Recession~~Relationships between recession parameters ~~to~~and event~~ and~~ /landscape variables

To capture how rainfall forcing affects streamflow recession, correlation analyses were performed. The correlation coefficients ~~of~~between recession parameters ~~to~~and event-associated variables are shown in Fig. 5 and Table ~~1 to capture how hydrometric forcing affects recession.~~2. The total precipitation (P), duration (D), total streamflow (Q_{tot}), antecedent streamflow (Q_{ant}~~)~~), and runoff coefficient (Q_{tot}/P) ~~are~~were negatively correlated ~~to~~with the recession coefficient, a. The average precipitation intensity (I_{avg}) and peak flow (Q_p), both of which represent the rainstorm magnitude, ~~are~~were not ~~significant~~significantly correlated to a. As for initial event conditions, ~~simply defined as~~ the 7-day antecedent precipitation, AP_{7day}, ~~is~~defined as the seven-day rainfall amount prior to a rainstorm, was not correlated to ~~the a;~~, nor were other AP period lengths ~~of AP~~ (3-, 5-, 14-, and 30-day~~) also show insignificant correlation to a. Notably, Q_{ant} is negatively correlated to a.~~). Unlike the recession coefficient, which was strongly ~~depends~~dependent on the hydrometric variables, nonlinearity, b, ~~is only~~ was only correlated with two, Q_{ant} and Q_p, with positive ~~to Q_{ant}. It indicated~~and negative correlations, respectively. This indicates that higher antecedent flow could lead to higher nonlinearity~~. A little surprise is that the nonlinearity is statistically negative to~~ and peak flow ~~(Q_p), presenting the nonlinearity decreases with rainstorm magnitude. To summarize from the view of the aggregated dataset~~to lower. Overall, hydrometric forcing moderately controls the coefficient and only slightly ~~involves~~affects nonlinearity.

~~On our 19 catchments,~~ Regarding landscape variables, the average height (H), length (L~~)~~), and gradient (G) of the flow-path ~~are~~were approx. 120 m, 252 m, and 0.47, respectively (Table S2). ~~Basically, those flow-path associated parameters are highly dependent. Thus, we used L/G, which has been proven highly correlated to water residence time (McGuire et al., 2005; Seybold et al., 2017), as a proxy presenting the interaction of landscape and climate, is~~The mean L/G value for our catchments was approx. 951m. Forest ~~is~~was the dominant landscape type, and the average forest coverage ~~is~~was approx. 67.1~~% with a range~~%, ranging between 11.8-92.1%. Notably, the catchments in the western plain are characterized by gentle gradients of flow-path, such as catchments W8, W9, W11, W12, W13, and W14. Due to the gentle landscape and higher L/G, agricultural activities are the dominant land cover in those catchments. The details of the landscape variables ~~could~~can be ~~referred to~~found in Table ~~S1~~S2.

The correlations ~~between~~of recession parameters against ~~event and~~ landscape variables are illustrated in Fig. 5 and Table ~~1~~2. Most landscape variables (*H*, *L*, *G*, *L*/*G*, *DD*, S_m, *HI*, C_W, C_F, and C_A) are significantly correlated ~~to~~with the coefficient, particularly ~~for~~ the flow-path-associated ones (*H*, *L*, *G*, *L*/*G*, and *DD*). ~~The flow-path-associated variables, such as flow~~Flow-path height (*H*), length (*L*), and gradient (*G*~~), are~~) were negatively correlated to the ~~coefficients~~coefficient, but ~~positive to~~ *L*/*G* and *DD*~~. Besides, that coefficient increases with the decrease of S_m shows that quick recession occurs in a catchment with gentle gradient. In contrast~~ were positively correlated. Additionally, the coefficient increases ~~with~~as *HI*~~, showing a sharp recession in actively eroded catchments. Moreover~~ and S_m decrease. Looking at land cover, the coefficient increases with C_W (~~fraction~~proportion of water body ~~area~~land cover) and C_A (~~fraction~~proportion of agriculture ~~area~~land cover) and decreases with C_F (~~fraction~~proportion of forest ~~area). A catchment with more~~land cover). Greater water~~ bodies~~ body and/or agricultural ~~lands leads~~land area in a catchment lead to a faster recession, yet ~~a catchment with more forest lands could reduce the recession coefficient.~~greater forested land area can slow recession. Correlations between *b* and the landscape variables were generally weaker and of the opposite sign than the correlations seen with *a*. There were also less significant correlations. In short, most landscape variables are ~~highly~~moderately associated with ~~the coefficient and only a few, such as *HI* and *A* are slightly negative to~~ the coefficient and low-to-moderately with nonlinearity. ~~Yet~~Perhaps, putting all catchments with various landscape features together ~~may~~would obscure the landscape's control in recession~~ coefficient and nonlinearity~~.

4. Discussion

4.1 Recession parameters in ~~subtropical~~small mountainous ~~catchments~~rivers

Notably, the parameters derived from the point-cloud and individual segments exhibit distinct systematic biases (Fig. 4). The larger *a* and smaller *b* values derived from the point-cloud than from individual segments could be expected since the flood distribution is right-skewed, representing a large number of small cases with scarce extremes. The point-cloud-derived nonlinearity *b* could be altered either by the numerous small cases or the scarce extreme cases during fitting. Jachens et al. (2020) indicated that the event properties (variation among inter-event, storm magnitude, and antecedent condition) strongly affect parameter estimation. Since *a* and *b* are inherently dependent and while the decorrelation method might be valid for some specific cases (Biswal, 2021), the way (e.g. fixing *b*) to obtain the *a* or *b* of an individual event is still goal-dependent (Sharma and Biswal, 2022). Even so, using the median from individual segments is suggested, compared to the point-cloud derivation (Dralle et al., 2017; Jachens et al., 2020).

The recession coefficients observed in our small mountainous rivers varied across a wide range ~~of recession coefficient from our 19 catchments is~~ (from 0.~~010~~003 to 0.~~290, comparable with values in the literature, for example,~~ 273 hr^{-1}), which is similar to ranges seen in other studies, such as 0.012~~ to ~~–0.230 for Swedish catchments (Bogaart et al., 2016) and 0.015~~ to ~~–0.171 for ~~USA~~ watersheds in the USA (Biswal and Marani, 2010). Higher median recession coefficients ~~are~~were found in W8, W11, W12, and W14, where which we attributed to the landscape features of shorter- and steeper gentler flow paths, i.e., dense drainage networks, are the main landscape features.. By contrast, catchments with longer- and gentle steeper flow paths, such as W7 and W15, have lower median recession coefficients. It indicates that Taken together, these data demonstrate how landscape structure (e.g., particularly drainage density and flow-path-associated variables) could, can affect the recession coefficient, as. The findings presented in Table 2 shows.corroborate this (discussed more in Sect. 4.2). On the other hand, the median of recession nonlinearity, *b*, is approx. 1.669 (Fig. 3b) with a range of 0.690 to 3.0, which are4.39, also comparable withto the ranges found in the literature. For example, values of *b* from 0.5 to 2.1 could be found in 220 Swedish catchments with low--flow data (Bogaart et al., 2016), 0.6 to 1.7 for 22 Taiwanese rivers derived from low-flow data (Yeh and Huang, 2019), and 1.5 to 3.2 for 67 USA watersheds with event data (Biswal and Marani, 2010). Non-linear storage-outflow relationshiprelationships (*b* is not equal to 1.0) isare prevalent for most catchments worldwide. In our cases, the highest and lowest median values of *b* arewere found in W7 and W19, respectively. Catchment W7 with high channel slope and flow-path gradient (Table S1), presents higher non-linear storage-outflow. W19, by contrast, hasDespite the fact that these two catchments have similar landscape settings with W7, but has the lowest.structures, their recession nonlinearity exhibits distinct differences. Perhaps, other controlling factors, such as geological structure (i.e., connectivity between the deep aquifer and the stream, heterogeneous hydraulic properties, and/or the interface slope between the shallow and bedrock layers, see Roques et al., 2022) or land cover, (Tague and Grant, 2004), might regulate thealter recession behavior (Tague and Grant, 2004).as well.

Notably, a distinct systematic bias is found between the nonlinearity derived from individual segments and the aggregated point-cloud (Fig. 4). Smaller *b* value derived from the aggregated point-cloud than that from individual segments could be expected since the flood distribution is right-skewed; that is, large number of small cases with scarce extremes. Nonlinearity *b* derived from aggregated point-cloud is synthesized from all points, which could be altered either by the numerous small cases or the scarce extreme cases as fitting. The median from aggregated point-cloud is more or less like the way of the master recession curve. Jachens et al. (2020) indicated that the event properties (variation among inter-event, storm magnitude, and antecedent condition) strongly affect the parameter estimation. In this regard, it suggested that using the median from individual segments to represent the central tendency of a collection of recession segments (Dralle et al., 2017; Jachens et al., 2020), but the way to obtain the b is still goal-dependent (Sharma and Biswal, 2022).

4.2 Landscape structure controls on the median of recession parameters

Landscape structure aggregates catchment hydraulic properties, embodying recession parameters conceivablyconceptually. Therefore, recession behaviors in a catchment could be interpreted from two perspectives:, hillslope hydraulics and inter-hillslope heterogeneity (Harman et al., 2009), both of which mightcould be represented by the flow-path-associated variables (e.g., *H*, *L*, *G*, *L*/*G*, and *DD* in Table 12) and drainage area. Notably, heterogeneity may increase with catchmentdrainage area because of the possibility of including a wider range of subsurface conditions. Two studies, for example, investigated the recession behaviors in two small forested catchments (68 km^2 in Mahurangi, New Zealand, McMillan et al., 2014 and 41 ha in Panola Mountain Research Watershed, USA, Clark et al., Recession2009; Harman et al., 2009) and found that recession nonlinearity ~~increases~~might also increase with drainage area because a larger area accommodates more possibility of superimposition of multiple linear reservoirs, which has been seen in the 68 km2 Mahurangi watershed, New Zealand (McMillan et al., 2014), and the 41 ha Panola Mountain Research Watershed, USA (Clark et al., 2009; Harman et al., 2009), though this does not appear to be the case in our study (Fig. 6a).~~.~~

~~Correlation~~The correlation analysis ~~elucidates~~showed that flow-path-associated variables (*H*, *L*, *G*, *L*/*G*, *DD*) only have a vague correlation with the recession nonlinearity (~~Fig.~~ Table 2). This could have two explanations: First~~6a). It might be explained by: first~~, some of our catchments are much larger than 500 km^2, which far exceeds the extent of common rainstorms (usually less than 200 km^2). In ~~those~~these large catchments, the limited extent of ~~rainstorm~~rainstorms would not bring about a comprehensive recession response in the outflow hydrograph (Huang et al., 2012). Second, the drainage area cannot reflect the unknown number of aquifers (Ajami et al., 2011). Moreover, Karlsen et al. (2019) argued that the dependence of *b* on landscape variables would change with the streamflow rate. Specifically, ~~the variable~~flow-path height, *H*, dominates the nonlinearity during high flow, whereas the ~~variable,~~ drainage area, *A*, gains more importance during low ~~flows~~flow. The relationship between flow-path-associated variables and drainage area ~~against~~and recession needs to be ~~further~~ examined in our catchments.

4.2.1 Landscape structure ~~to~~controls on recession coefficient~~,~~ *a*

~~The significance~~Since different combinations of landscape ~~variables might be altered by drainage area, which~~structure and rainstorm characteristics might result in ~~an opposite~~diverse recession ~~response. Further, in our cases, catchment area~~responses and drainage area could not solely ~~and significantly~~ explain ~~the~~our recession behaviors (Fig. 6a~~). The~~), the flow-path-associated variables ~~were tried to correlate with~~and drainage area ~~and~~ were used to classify the catchments. Surprisingly, an inverse relationship between the *L*/*G* ratio ~~against~~and drainage area emerged ~~surprisingly~~ (Fig. 6b). The *L*/*G* ratio, a measure of the distribution of flow-path length over gradient at a catchment scale ~~(McGuire et al., 2005),~~, is highly correlated to *DD* and the topographic wetness index (Beven and Kirkby, 1979). Therefore, *L/G* is apt to ~~present~~represent the hillslope hydraulics at a catchment scale. In Fig. 6b, all catchments could be simply classified into three types: type A ~~is~~are large catchments (area > 500 km^2), B ~~is~~are small catchments with low *L*/*G*, and C ~~is~~are small catchments with high *L*/G. ~~The~~Another correlation analysis was performed between these parameters and the flow-path-associated variables (*H*, *L*, *L*/*G*, and *DD*) ~~are re-applied onto the recession parameters~~ according to ~~this classification~~these classifications (Fig. 7). ~~As expected, the~~ The recession coefficients ~~correlate~~correlated with the flow-path-associated variables~~.~~ in small catchments (Type B and C only) significantly. Flow-path height, *H*, is directly linked to the water table depth ~~under~~in the ~~relatively~~ homogeneous hillslopes. ~~Hence,~~A steeper hillslope corresponds to permeable soils with higher *H*, leading to a deeper and longer groundwater flow system and slower drainage (Karlsen et al., 2019). ~~The high~~High *DD* and short *L* lead to a higher recession coefficient due to shorter flow paths. Additionally, McGuire et al. (2005) ~~demonstrated~~used isotopic evidence to ~~prove~~demonstrate that the ~~transit~~residence time increases with *L* in Oregon, USA. In our case, both *DD* and *L/G* (Fig. 7a-c) confirm ~~the~~these documented relations.

CatchmentsSmall catchments with high *DD* or *L/G*, which represent a denser stream network (high *DD*) and/or short-and-gentle hillslopes, (high *L/G*), have a higher recession coefficient.

Appeal to existing theories, flow-path variables could be regarded as the aggregation of aquifers with various geometries, or vertical heterogeneity of aquifer (Rupp and Selker, 2006). Flow-path variables L, H, G can be the proxy of *Bcosϕ*, *Bsinϕ+Dcosϕ*, and *D/B+tanϕ*, respectively. Large *B* and *tanϕ* aquifers have a small coefficient *a* (Fig. 3 in Rupp and Selker, 2006, where B, D, ϕ indicate the length, depth, and slope of the aquifer, respectively). Our inverse relationship between *H* and *a* confirms that the hydraulic parameters vary markedly with depth (Rupp and Selker, 2006).

4.2.2 Landscape structure tocontrols on recession nonlinearity, *b*

The recession nonlinearity conditionally responds to landscape structure (Fig. 7e-7h). If Type A catchments (large area with low *L/G*, gray solid dots in Fig. 7) are excluded, all flow-path-associated variables become statistically significantsignificantly correlated with nonlinearity. The positive relationship of *b* with *H* and *L* indicates that steeper and rougher hillslopehillslopes present non-linear recession behaviour. Withbehavior. Perhaps with the increase of flow-path length *L*, subsurface runoff has more chances of flowing through various blocks (e.g., temporarily perched groundwater). The two composite indices, *DD* and *L*/*G*, are negatively related to the value of *b* (Fig. 7g-h), perhaps because that short). Short-and-gentle hillslopes lead to a larger saturation area (Bogaart et al., 2016; Sayama et al., 2011). The), and the expansion of the saturation area indicates that the whole subsurface is gettingbecomes saturated and connected andwell, thus reducesreducing heterogeneity. It suggested that the *L/G* ratio affects the nonlinearity significantly for small catchments; however, it is not valid forthe cases of our large catchments, which necessitates further theory developmentinterpretation associated with scale.

4.3 Rainfall amount controls on the variation of recession parameters

Recession behavior is a convolutional response starting as rainfall fallingrain falls within catchments. Thus, we separately examined the recession parameters against hydrometric variables for the three catchment types (Types A, B, and C) to rule out the influences (Fig. 8). Two This produced two significant findings are: (1) the recession coefficient, *a*, decreases with the rainfall amount in all types; and (2) the recession nonlinearity, *b*, shows oppositecontrasting responses in Type A and B (Type C is statistically insignificant). The parameter, *b*, inIn heterogeneity-dominated (large) or hydraulics-dominated (small and steep) catchments would increase, *b* increases or decreasedecreases with rainfall amount, respectively. The contrasting recession responses are further discussed in the following two sections.

4.3.1 Rainfall amount controls on recession coefficient, *a*

Several empirical studies found a positive or independent relationship between coefficient, *a* and streamflow; for example, Santos et al. (2019) found that higher streamflow hasproduced a largergreater *a* value, reflecting a quick recession in Switzerland's catchments. In Sweden, annual rainfall variation might be independent of the *a* (Bogaart et al., 2016). However, most studies found a negative relationship between a and storage measures (Table 1). For instance, Biswal and Nagesh Kumar (2014) found a negative correlation between a and the antecedent flow rate, while Ghosh et al. (2015) found that high peak flow events tend to produce a small value of a. In our study of three catchment types, recession coefficients decreased with rainfall amount in all catchment types (Fig. 8a-c). Harman's virtual experiments et al. (2009) demonstrated that the recession coefficient is determined by the tension between can be expressed as $a = V_0/R^{b-1}$ (where V_0 and R represent the recharge rate and the spatial heterogeneity of storage and flow mean of the velocity (Hamann et al., 2009). In our three catchment types, recession coefficients decrease with rainfall amount (Fig. distribution of hillslope flow and8a-c). It may infer that the huge rainfall brought by typhoons may overwhelm the rate, respectively). In the case of heavy rainfall, the increase of R is much larger than that of V_0. The effect of this disproportionate rainfall input increase on a could offset the increase in flow velocity, resulting in a slowernegative correlation. Moreover, Biswal and Nagesh Kumar (2014) used a geomorphological recession in large rainstorms. Interestingly, Type C has a higher intercept of the rainfall-a relationship likeflow model $a \propto c/q^{b-1}$ (where c and q represent the theorical curve of $h_0/D=1$ (Rupp and Selker, 2006), suggesting that celerity and rate of channel flow, respectively, and which is similar to Harman's theory) to explain why "a" is negatively correlated with "q." To sum up, the lower H of type C tends to be saturated and have a quick recession. negative correlation between coefficient a and rainfall amount (e.g. peak flow and prior soil moisture) is consistent with the literature and is prevalently in most regions (also see Table 1).

4.3.2 Opposite controlOpposing controls of rainfall on recession nonlinearity, *b*

TheLiterature covering the variation of recession nonlinearity among events is divergent. Some studies concluded that nonlinearity, b, is controlled by landscape structure and is static or is insensitive to rainfall (Biswal and Marani, 2010; Brutsaert and Nieber, 1977; Dralle et al., 2017). In other studies, nonlinearity, b, decreases with streamflow rate, albeit on different temporal scales (Shaw and Riha, 2012; Karlsen et al., 2019; Santos et al., 2019). Although someSome studies have even argued that the nonlinearity can change over the course of an event dynamically (Rupp and Selker, 2006; Luo et al., 2018), this study treated b as a constant and the inter-event variability is discussed as the following.; Roques et al., 2022). In our study, nonlinearity b presentsshowed a positive, flat, negative, and flat relationship with rainfall in Type A, B, and C catchments, respectively (Fig. 8d-f). A possible interpretation is that the short-and-gentle catchmentsSmall catchment areas (Type B and C catchments) have a wide range of contributing area, which expands with may be explained by a 2-dimensional hillslope model (Roques et al., 2022). During heavy rainfall quickly. The pervasive saturation overland, when fast flow reducespathways are activated, the nonlinearity of recession. With the connection of saturated zones, the large storms can activate different draining sources, mixing them downstream and result in the would decrease of b (as. Type B catchments (Steep slopes) with more heterogeneous hydraulic conductivity would experience larger changes in recession nonlinearity, whereas Type C demonstrated). On the contrarycatchments (gentle slopes) with more homogeneous hydraulic conductivity would experience smaller changes in recession nonlinearity. Conversely, the nonlinearity, b, increases with the rainfall amount in Type A catchments. In large and heterogeneous catchments, the expansion of the contributing area is less steady and more~~ unsteady and~~ complicated, and thus the nonlinearity increases with rainfall amount. ~~The nonlinearity increases with the heterogeneity within a large catchment (Harman et al., 2009). The~~A contrasting response of *b* to rainfall similar to the one seen in this study was ~~only~~also found in Biswal and Nagesh Kumar (2013), which attributed it to the change in subsurface flow contributions along the channel that affect the response direction ~~response~~ of *b*. Our study revealed that landscape structure and rainfall amount ~~dominate~~control the direction and magnitude of recession response, respectively. Future research ~~direction~~ could further consider different landscape structures ~~into modelling~~when modeling the intra-event variation of *b*.

4.4 Landscape structure regulates recession ~~patterns~~behavior

The above two sections ~~elucidate~~have demonstrated the ~~role~~influence of landscape and rainfall amount ~~in~~on streamflow recession ~~behaviors~~behavior. Thus, a ~~hypothesis~~perceptual model which demonstrates the interactive regulation of landscape structure and rainfall amount on recession nonlinearity is introduced (Fig. 9). Landscape structure is considered ~~from~~in two ~~dimensions in terms of~~contexts, spatial heterogeneity (drainage area) and hillslope ~~hydraulic, which are, respectively, represented by drainage area and~~ hydraulics (*L*/G~~. While the~~). The drainage area ~~might~~may correlate to the number of perched storages within the catchments, and the *L/G* ~~featured by short-and-gentle~~ratio, encapsulating hillslope ~~indicates that~~geometry, can indicate the ~~size~~dynamics of the contributing area associated with runoff generation.

Along the spatial heterogeneity dimension (from Type B to A, with increasing drainage area), additional perched storages respond increasingly with rainfall amount and thus enhance the recession nonlinearity. Perched storages are ~~inclined~~expected to occur where the hydrological conductivity abruptly decreases due to heterogeneous soil properties or geological ~~structure~~structures. The existence of perched storages was found in an experimental forested catchment in Taiwan ~~by~~through an intensive ~~pore~~soil water monitoring scheme (Liang, 2020). Large catchments ~~might have more perched storages, and consequently~~may suffer uneven spatial rainfall~~ activate~~, which activates perched storages locally, and thus, the nonlinearity increases. On the other hand, along the *L*/*G* dimension (increasing from Type B to C), the ~~accumulated~~heterogeneities of hydraulic conductivities decrease. Heavy rainfall~~ expands~~, causing saturation ~~zone quickly, which prefers~~ and expansion of the ~~generation of~~ saturation ~~excess overland flow. With~~area, can mediate the ~~increase of *L/G*, the runoff generation varies from subsurface runoff to overall saturation excess overland flow, and thus decreases~~heterogeneity of hydraulic conductivity and thereby reduce nonlinearity.

5. Summary

Streamflow recession, which reflects the rainfall-runoff process after rainstorms, is crucial for baseflow ~~estimation and~~ assessment. This study investigated the ~~recession responses to~~effects of landscape structure and rainfall amount ~~through~~on recession using power-law recession ~~from~~analysis for 291 ~~catchment~~rainfall events~~.~~ in small mountainous rivers. Despite the power-law equation being widely used, different procedures of segment extraction, starting point selection, selection of the procedure ofpoint-cloud or individual segment fitting method, fitting details, and so on usually result in considerably disparate and inconsistent parameter estimation estimations. This implies that it is diverse and of considerable inconsistency. For example, the selection of not possible to infer recession segments predominatescharacteristics by comparing the parameters found in the literature. The coefficient and nonlinearity significantly and leads to controversy, which makes the inter-comparison among studies complicated and delivers biased inference.derived from point-cloud are considerably larger and smaller, respectively, than the median of individual segments.

In our cases, landscape structure, mainly *DD* or *L/G*, and is moderately correlated to coefficient, but only modestly to nonlinearity. If classifying the catchments in accordance with spatial heterogeneity (drainage area) and hillslope hydraulics (*L*/G), the coefficient increases with *L*/*G* and nonlinearity decreases with *L*/*G* significantly in small catchments. This likely reveals that both spatial heterogeneity and hydraulic properties regulate recession simultaneously. Along the hillslope hydraulics dimension, small catchments with high *L/G* attributed to their short-and-gentle hillslopes, have higher recession coefficients. Additionally, *L*/*G* is negatively correlated to nonlinearity for small catchments, perhaps because short-and-gentle hillslopes can expand saturation area and connect different aquifers easily, thus reducing nonlinearity. Note that *a* and *b* are inherently dependent, so some uncertainty might be involved. Even so, both parameters, whether derived using the point-cloud or individual segments (Fig. 4), present similar fluctuations among catchments, which supports our arguments.

Further, rainfall amount playalso plays a dominant rolesrole in estimating recession coefficient. The coefficient increases with the increase of *DD* or *L/G*, indicating catchments with dense networks or more short-and-gentle hillslopes would lead to a higher coefficient. Surprisingly, it parameter *a*. It decreases with rainfall amount; probably the large rainfall develops saturated zones connectivity, resulting in more water from slow reservoirs and drained slowly. The diverse for all catchments. On the other hand, contrasting response directiondirections of nonlinearity likely depends onto rainfall amount could be found along the dimension of spatial heterogeneity (drainage area) and L/G, respectively. The more heterogeneous catchments give rise to the increase in the recession nonlinearity. On the contrary,). Larger catchments with gentle slopes could expand contributing area easily, and then generate saturation overland flow pervasively and thus reduceexhibited an increase in recession nonlinearity. with higher rainfall, whereas smaller catchments showed a decrease in recession nonlinearity with higher rainfall. Conjointly, our hypothesis presents an an interactive regulation of recession by landscape structure and rainfall amount to recessionwas proposed. In sum, landscape structure which has different preferences of recession mechanism(spatial heterogeneity and hillslope hydraulics) may determine the recession behavior via various aquifer settings, and the rainfall amount tunes the magnitude of recession nonlinearity apparently. If the hypothesisperceptual model is valid, two challenges should be addressed further. First, the alteration of contrasting response direction inof nonlinearity to rainfall, depending on the predominance betweenof spatial heterogeneity and L/G necessitates, requires further theoretical validation further. Clarifying which environmental factors could presentrepresent the spatial heterogeneity and hillslope hydraulics is also an arduous task but is crucial for recession estimation. Second, the careful determination of the response direction of nonlinearity is crucial to the regional recession assessment, particularly for climatic scenarios. . An incorrect direction would strongly affect the ~~inference.~~ interpretation, particularly for climatic scenarios. Validating the landscape structure control in ~~different regions~~rainstorm scale would aid in completing the understating of recession variations.

Data availability. Hourly streamflow data can be obtained from Taiwan Water Resource Agency and Tai-Power company. The authors declare that data supporting the findings of this study are accessible from the article and its supplementary materials.

Author contributions. Conceptualization and Methodology: JYL and JCH. Data Curation and Validation: TYL. Formal analysis: JYL and CJY. Investigation and Writing – Original Draft: JYL. Writing – Review and Editing: JCH and TRP.

Competing interests. The authors claim no potential competing interests

Acknowledgements. This research was funded by the Ministry of Science and Technology, Taiwan (110-2811-M-005-509, and 109-2811-B-002-631) and the NTU Research Center for Future Earth (107L901004). J. Y. Lee and C. J. Yang was supported by the grants from Ministry of Science and Technology, Taiwan (110-2811-M-005-521, 110-2917-I-564-009).

References

Ajami, H., Troch, P. A., Maddock III, T., Meixner, T., and Eastoe, C.: Quantifying mountain block recharge by means of catchment-scale storage-discharge relationships, Water Resour. Res., 47, W04504, https://doi.org/10.1029/2010WR009598, 2011.

Beven, K. J. and Kirkby, M. J.: A physically based, variable contributing area model of basin hydrology, Hydrol. Sci. J., 24, 43–69, https://doi.org/10.1080/02626667909491834, 1979.

Biswal, B. and Marani, M.: Geomorphological origin of recession curves, Geophys. Res. Lett., 37, L24403, https://doi.org/10.1029/2010GL045415, 2010.

Biswal, B. and Nagesh Kumar, D.: Study of dynamic behaviour of recession curves, Hydrol. Process., 28, 784–792, https://doi.org/10.1002/hyp.9604, 2014.

Biswal, B., and Nagesh Kumar, D.: A general geomorphological recession flow model for river basins. Water Resour. Res., 49(8), 4900-4906, https://doi.org/10.1002/wrcr.20379, 2013.

Biswal, B.: Decorrelation is not dissociation: there is no means to entirely decouple the Brutsaert-Nieber parameters in streamflow recession analysis, Adv. Water. Resour., 147, 103822, https://doi.org/10.1016/j.advwatres.2020.103822, 2021.
~~. and Nagesh Kumar, D.: Study of dynamic behaviour of recession curves, Hydrol. Process., 28, 784–792, https://doi.org/10.1002/hyp.9604, 2014.~~

Bogaart, P. W., Van Der Velde, Y., Lyon, S. W., and Dekker, S. C.: Streamflow recession patterns can help unravel the role of climate and humans in landscape co-evolution, Hydrol. Earth Syst. Sci., 20, 1413–1432, https://doi.org/10.5194/hess-20-1413-2016, 2016.

Brutsaert, W. and Nieber, J. L.: Regionalized drought flow hydrographs from a mature glaciated plateau, Water Resour. Res., 13, 637–643, https://doi.org/10.1029/WR013i003p00637, 1977.

Brutsaert, W.: Hydrology: an introduction, Cambridge university press, https://doi.org/10.1017/CBO9780511808470, 2005.

Brutsaert, W.: Long-term groundwater storage trends estimated from streamflow records: Climatic perspective, Water Resour. Res., 44, W02409, https://doi.org/10.1029/2007WR006518, 2008.

~~Brutsaert, W. and Nieber, J. L.: Regionalized drought flow hydrographs from a mature glaciated plateau, Water Resour. Res., 13, 637–643, https://doi.org/10.1029/WR013i003p00637, 1977.~~

Clark, M. P., Rupp, D. E., Woods, R. A., Tromp-van Meerveld, H., Peters, N., and Freer, J.: Consistency between hydrological models and field observations: linking processes at the hillslope scale to hydrological responses at the watershed scale, Hydrol. Process. Int. J., 23, 311–319, https://doi.org/10.1002/hyp.7154, 2009.

Dralle, D. N., Karst, N. J., Charalampous, K., Veenstra, A., and Thompson, S. E.: Event-scale power law recession analysis: quantifying methodological uncertainty, Hydrol. Earth Syst. Sci., 21, 65–81, https://doi.org/10.5194/hess-21-65-2017, 2017.

Dralle, D., Karst, N., and Thompson, S. E.: a, b careful: The challenge of scale invariance for comparative analyses in power law models of the streamflow recession. Geophys. Res. Lett., 42(21), 9285-9293, https://doi.org/10.1002/2015GL066007, 2015.

~~Dralle, D. N., Karst, N. J., Charalampous, K., Veenstra, A., and Thompson, S. E.: Event-scale power law recession analysis: quantifying methodological uncertainty, Hydrol. Earth Syst. Sci., 21, 65–81, https://doi.org/10.5194/hess-21-65-2017, 2017.~~

Harman, C. J., Sivapalan, M., and Kumar, P.: Power law catchment-scale recessions arising from heterogeneous linear small-scale dynamics, Water Resour. Res., 45, W09404, https://doi.org/10.1029/2008WR007392, 2009.

Huang, J.-C., ~~Yu, C.-K., Lee, J.-Y., Cheng, L.-W., Lee, T.-Y., and Kao, S.-J.: Linking typhoon tracks and spatial rainfall patterns for improving flood lead time predictions over a mesoscale mountainous watershed, Water Resour. Res., 48, W09540, https://doi.org/10.1029/2011WR011508, 2012.~~

~~Huang, J.-C.,~~ Lee, T.-Y., and Lee, J.-Y.: Observed magnified runoff response to rainfall intensification under global warming, Environmental Research Letters, 9, 034008, https://doi.org/10.1088/1748-9326/9/3/034008, 2014.

Huang, J.-C., Lee, T.-Y., Lin, T.-C., Hein, T., Lee, L.-C., Shih, Y.-T., Kao, S.-J., Shiah, F.-K., and Lin, N.-H.: Effects of different N sources on riverine DIN export and retention in a subtropical high-standing island, Taiwan, Biogeosciences, 13, 1787–1800, https://doi.org/10.5194/bg-13-1787-2016, 2016.

Huang, J.-C., Yu, C.-K., Lee, J.-Y., Cheng, L.-W., Lee, T.-Y., and Kao, S.-J.: Linking typhoon tracks and spatial rainfall patterns for improving flood lead time predictions over a mesoscale mountainous watershed, Water Resour. Res., 48, W09540, https://doi.org/10.1029/2011WR011508, 2012.

Jachens, E. R., Rupp, D. E., Roques, C., and Selker, J. S.: Recession analysis revisited: impacts of climate on parameter estimation, Hydrol. Earth Syst. Sci., 24, 1159–1170, https://doi.org/10.5194/hess-24-1159-2020, 2020.

Karlsen, R. H., Bishop, K., Grabs, T., Ottosson-Löfvenius, M., Laudon, H., and Seibert, J.: The role of landscape properties, storage and evapotranspiration on variability in streamflow recessions in a boreal catchment, J. Hydrol., 570, 315–328, https://doi.org/10.1016/j.jhydrol.2018.12.065, 2019.

Kirchner, J. W.: Catchments as simple dynamical systems: Catchment characterization, rainfall-runoff modeling, and doing hydrology backward, Water Resour. Res., 45, W02429, https://doi.org/10.1029/2008WR006912, 2009.

Lee, J.-Y., Shih, Y.-T., Lan, C.-Y., Lee, T.-Y., Peng, T.-R., Lee, C.-T., Huang, J.-C.: Rainstorm Magnitude Likely Regulates Event Water Fraction and Its Transit Time in Mesoscale Mountainous Catchments: Implication for Modelling Parameterization. Water, 12, 1169, https://doi.org/10.3390/w12041169, 2020.

Liang, W. L.: Dynamics of pore water pressure at the soil–bedrock interface recorded during a rainfall-induced shallow landslide in a steep natural forested headwater catchment, Taiwan. J. Hydrol., 587, 125003, https://doi.org/10.1016/j.jhydrol.2020.125003, 2020.

Luo, Z., Shen, C., Kong, J., Hua, G., Gao, X., Zhao, Z., Zhao, H., and Li, L.: Effects of unsaturated flow on hillslope recession characteristics. Water Resour. Res., 54(3), 2037-2056, https://doi.org/10.1002/2017WR022257, 2018

McGuire, K., McDonnell, J. J., Weiler, M., Kendall, C., McGlynn, B., Welker, J., and Seibert, J.: The role of topography on catchment-scale water residence time, Water Resour. Res., 41, W05002, https://doi.org/10.1029/2004WR003657, 2005.

McMillan, H., Gueguen, M., Grimon, E., Woods, R., Clark, M., and Rupp, D. E.: Spatial variability of hydrological processes and model structure diagnostics in a 50 km^2 catchment, Hydrol. Process., 28, 4896–4913, https://doi.org/10.1002/hyp.9988, 2014.

Mendoza, G. F., Steenhuis, T. S., Walter, M. T., and Parlange, J.-Y.: Estimating basin-wide hydraulic parameters of a semi-arid mountainous watershed by recession-flow analysis, J. Hydrol., 279, 57–69, https://doi.org/10.1016/S0022-1694(03)00174-4, 2003.

Millares, A., Polo, M. J., and Losada, M. A.: The hydrological response of baseflow in fractured mountain areas, Hydrol. Earth Syst. Sci., 13, 1261–1271, https://doi.org/10.5194/hess-13-1261-2009, 2009.

Palmroth, S., Katul, G. G., Hui, D., McCarthy, H. R., Jackson, R. B., and Oren, R.: Estimation of long-term basin scale evapotranspiration from streamflow time series, Water Resour. Res., 46, W10512, https://doi.org/10.1029/2009WR008838, 2010.

Roques, C., Rupp, D. E., and Selker, J. S.: Improved streamflow recession parameter estimation with attention to calculation of− dQ/dt. Adv. Water Resour., 108, 29-43, https://doi.org/10.1016/j.advwatres.2017.07.013, 2017

Rupp, D. E., and Selker, J. S.: On the use of the Boussinesq equation for interpreting recession hydrographs from sloping aquifers. Water Resour. Res., 42(12), https://doi.org/10.1029/2006WR005080, 2006.

Santos, A. C., Portela, M. M., Rinaldo, A., and Schaefli, B.: Estimation of streamflow recession parameters: New insights from an analytic streamflow distribution model, Hydrol. Process., 33, 1595–1609, https://doi.org/10.1002/hyp.13425, 2019.

Sayama, T., McDonnell, J. J., Dhakal, A., and Sullivan, K.: How much water can a watershed store?, Hydrol. Process., 25, 3899–3908, https://doi.org/10.1002/hyp.8288, 2011.

Seybold, H., Rothman, D. H., and Kirchner, J. W.: Climate's watermark in the geometry of stream networks. Geophysical Research Letters, 44(5), 2272-2280, https://doi.org/10.1002/2016GL072089, 2017.

Shaw, S. B. and Riha, S. J.: Examining individual recession events instead of a data cloud: Using a modified interpretation of dQ/dt–Q streamflow recession in glaciated watersheds to better inform models of low flow, J. Hydrol., 434, 46–54, https://doi.org/10.1016/j.jhydrol.2012.02.034, 2012.

Shiu, C., Liu, S. C., Fu, C., Dai, A., and Sun, Y.: How much do precipitation extremes change in a warming climate?, Geophys. Res. Lett., 39, L17707, https://doi.org/10.1029/2012GL052762, 2012.

Stölzle, M., Stahl, K., and Weiler, M.: Are streamflow recession characteristics really characteristic?, Hydrol. Earth Syst. Sci., 17, 817–828, https://doi.org/10.5194/hess-17-817-2013, 2013.

Tague, C. and Grant, G. E.: A geological framework for interpreting the low-flow regimes of Cascade streams, Willamette River Basin, Oregon, Water Resour. Res., 40, W04303, https://doi.org/10.1029/2003WR002629, 2004.

Vogel, R. M. and Kroll, C. N.: Regional geohydrologic-geomorphic relationships for the estimation of low-flow statistics, Water Resour. Res., 28, 2451–2458, https://doi.org/10.1029/92WR01007, 1992.

Yeh, H. and Huang, C.: Evaluation of basin storage–discharge sensitivity in Taiwan using low-flow recession analysis, Hydrol. Process., 33, 1434–1447, https://doi.org/10.1002/hyp.13411, 2019.

~~Seybold, H., Rothman, D. H., and Kirchner, J. W.: Climate's watermark in the geometry of stream networks. Geophysical Research Letters, 44(5), 2272-2280, https://doi.org/10.1002/2016GL072089, 2017.~~

Table 1: Summary of empirical recession ~~studies that investigated the dependence of recession parameters on environmental factors. Shade blue~~study results. Blue, red, and grey shades represent positive, negative, and no correlation with factors, respectively. ~~The label of number indicates~~Numbers inside cells correspond to the reference ~~number~~numbers in Table S1. The asterisk (*) represents this study.

Factor	Centrality of recession		Temporal variability of recession					
	Long-term		Inter-annual		Inter-seasonal		Inter-event	
	â	b	â	b	â	b	â	b
Climate/Moisture								
~~Annual rainfall~~Rainfall	1, 21	1 21	21	21			*	* * ~~—~~*
Maximum monthly rainfall		2						
Antecedent flow					4, 5		5, 13, 22, *	~~—~~*
Peak flow							8, * 6	19, * 19, * 8, *
Flow rate after peak							5, 6, 9 23	23
Total storage change						11		
Water table elevation					3	3		
Saturated area					3	3		
60 cm soil moisture					3	3		
Baseflow	1							
Evapotranspiration	1, 21	1 21			3, 12, 24	24 3		
Aridity index	16, 17, 21	15, 16, 17, 21						
Mean relative humidity		2						
Landscape								
Drainage area	10, 16, 20 1, *	1, 7, 16, 18, 24 20, *						
Long shape of catchment	10 *	~~—~~*						
Flow path height	*	24, *						
Flow path length	*	*						
Flow path gradient	*	*						
Mean elevation		2						
Standard deviation of elevation		2						
Catchment slope	17, 24	2, 17, 24						

Hypsometric integral	*	*				
Coefficient of variation of slope	16	16				
Topographic wetness index		2				
Ratio of flow-path length to gradient	*	*				
Drainage density	14, *	14				
	10	—*				
Subsurface flow contact time		2				
Landcover						
Reforestation			21	21		
Water management			21	21		
Plateaus coverage		15				
Young volcano rock coverage	14	14				
Forest coverage	18, *	—*				
Water bodies coverage	~~21~~*	16, 21, 24				
	21					
	16	—*				
Flood attenuation due to lakes	1	1				
Soil						
Soil depth		24				
Surface hydraulic conductivity	17	21				
	18	17				
Field capacity	16	16				
Moderate infiltration ~~rates soil~~rate soils		2				
Slow infiltration ~~rates soil~~rate soils		2				
Playas with impermeable soils		15				
Organic matter content		2				

Table 2: Spearman correlation coefficients between logarithmic hydrometric characteristics and recession characteristics for all ~~catchment-~~rainfall events at all catchments (n = 291). ~~Values in bold are~~Grey shades represent statistically significant ~~with~~at the 99% ~~level of~~ confidence level (p-value < 0.01).

Variable	Meaning	a [hr^{-1}]	b [-]
Hydrometric			
AP_{7day} [mm]	7-day antecedent precipitation	-0.080	0.010
P [mm]	Total precipitation	-0.524	-0.083
D [hr]	Duration of precipitation	-0.432	-0.054
I_{avg} [mm hr^{-1}]	Averaged precipitation intensity	-0.257	-0.026
Q_{tot} [mm]	Total streamflow	-0.609	-0.154
Q_{ant} [mm]	Antecedent streamflow	-0.339	0.266
Q_p [mm]	Peak flow	-0.247	-0.228
Q_{tot}/P [-]	Runoff coefficient	-0.337	-0.097
Landscape			
H [m]	Flow-path height	-0.491	0.224
L [m]	Flow-path length	-0.520	0.302
G [-]	Flow-path gradient	-0.453	0.189
L/G [m]	Ratio of flow-path length to gradient	0.470	-0.181
A [km^2]	Drainage area	0.040	-0.095
DD [km]	Drainage density	0.420	-0.217
S_m [%]	Gradient of ~~mainstream~~main stem	-0.318	0.229
HI [-]	Hypsometric integral	-0.498	0.226
ELO [-]	Basin elongation	-0.209	0.319
C_W [%]	Land cover - water bodies	0.330	-0.147
C_F [%]	Land cover - forest	-0.281	0.140
C_A [%]	Land cover - agriculture	0.268	-0.059

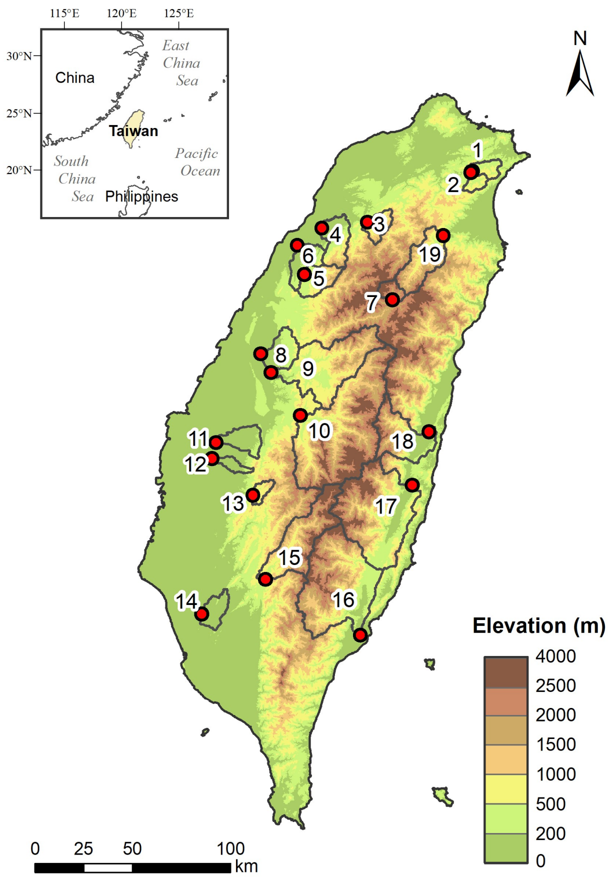

Figure 1: Topographic ~~distribution~~map of Taiwan and the locations of the selected catchments~~.~~ (red dots) and associated watersheds (outlines). The catchment ~~ID can be referred~~IDs correspond to ~~Table~~the IDs in Tables S2 and S3, in which the primary descriptions of hydrologic events and landscape variables are listed.

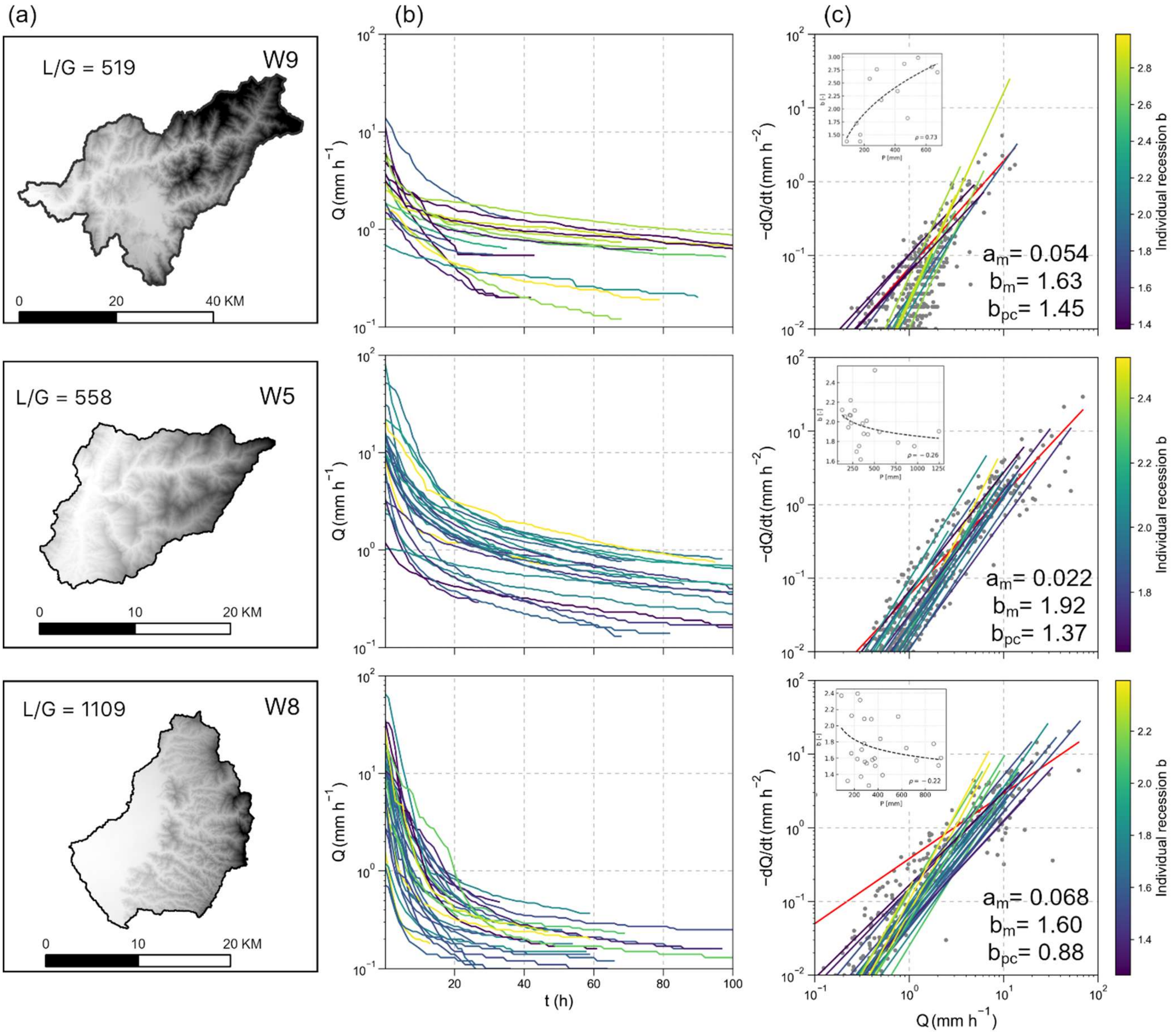

Figure 2: Landscape and recession plots for catchment W9 (row 1), W5 (row 2), and W8 (row 3). Landscape and flow-path topography (L/G) are shown in column (a). ~~The selected~~Selected recession segments from different rainstorms are shown in (b). Recession plots of all selected rainstorms are shown in column (c). The median of recession ~~parameter~~parameters *a* and b_m and the parameter b_{pc} derived from the point-cloud are shown in the lower-right corner. The recession *b* from individual ~~segment~~segments are colored from purple to yellow with increasing value of *b*, and the red line represents *b* derived using the point-cloud method.

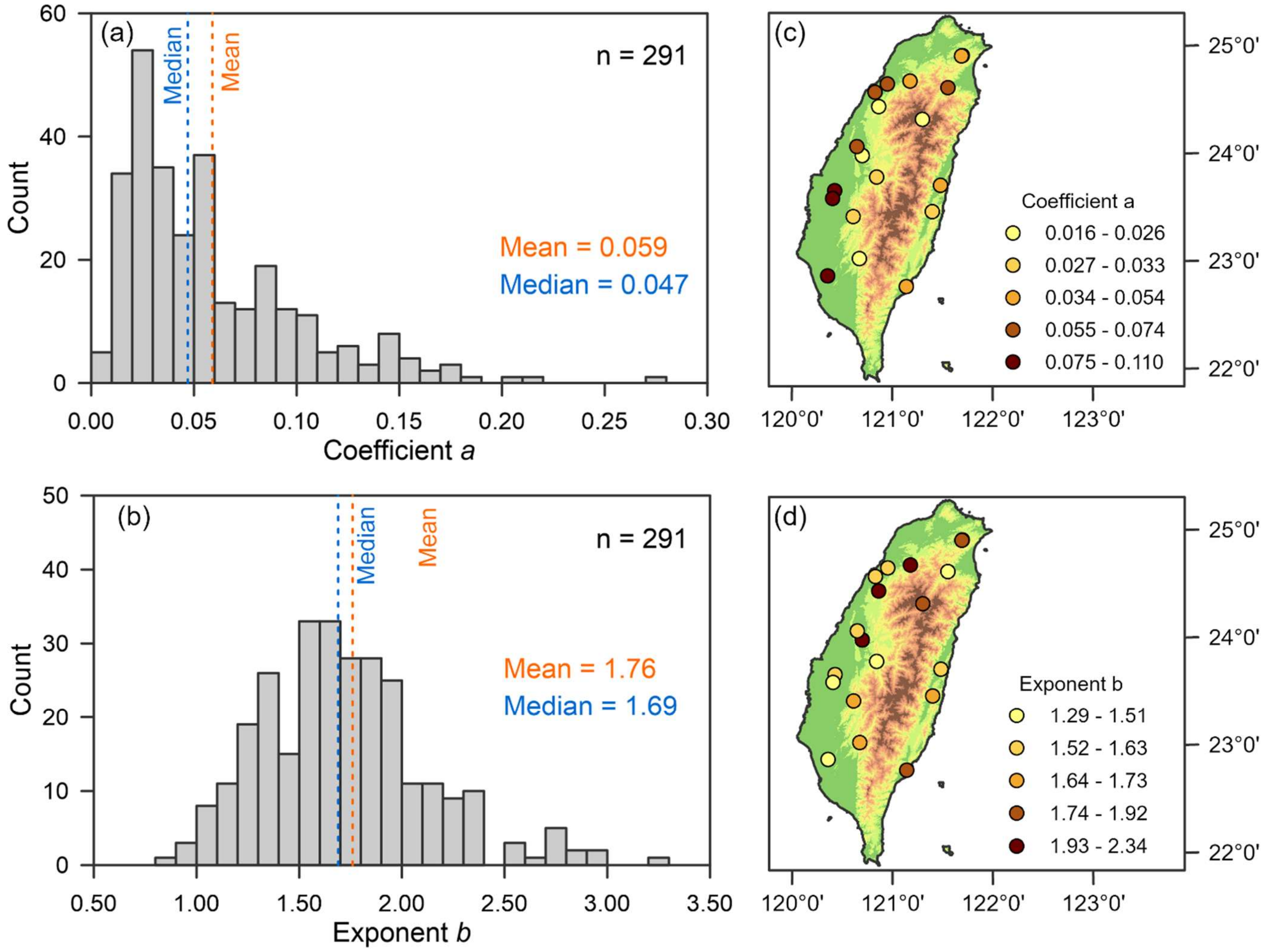

Figure 3: Distributions of recession parameterparameters *a* (a) and *b* (b) estimates in all catchment catchments and events. SpatialThe spatial distributions of the medians of parameterparameters *a* (c) and *b* (d). ColorsThe colors of dotthe dots represent the quantiles category.

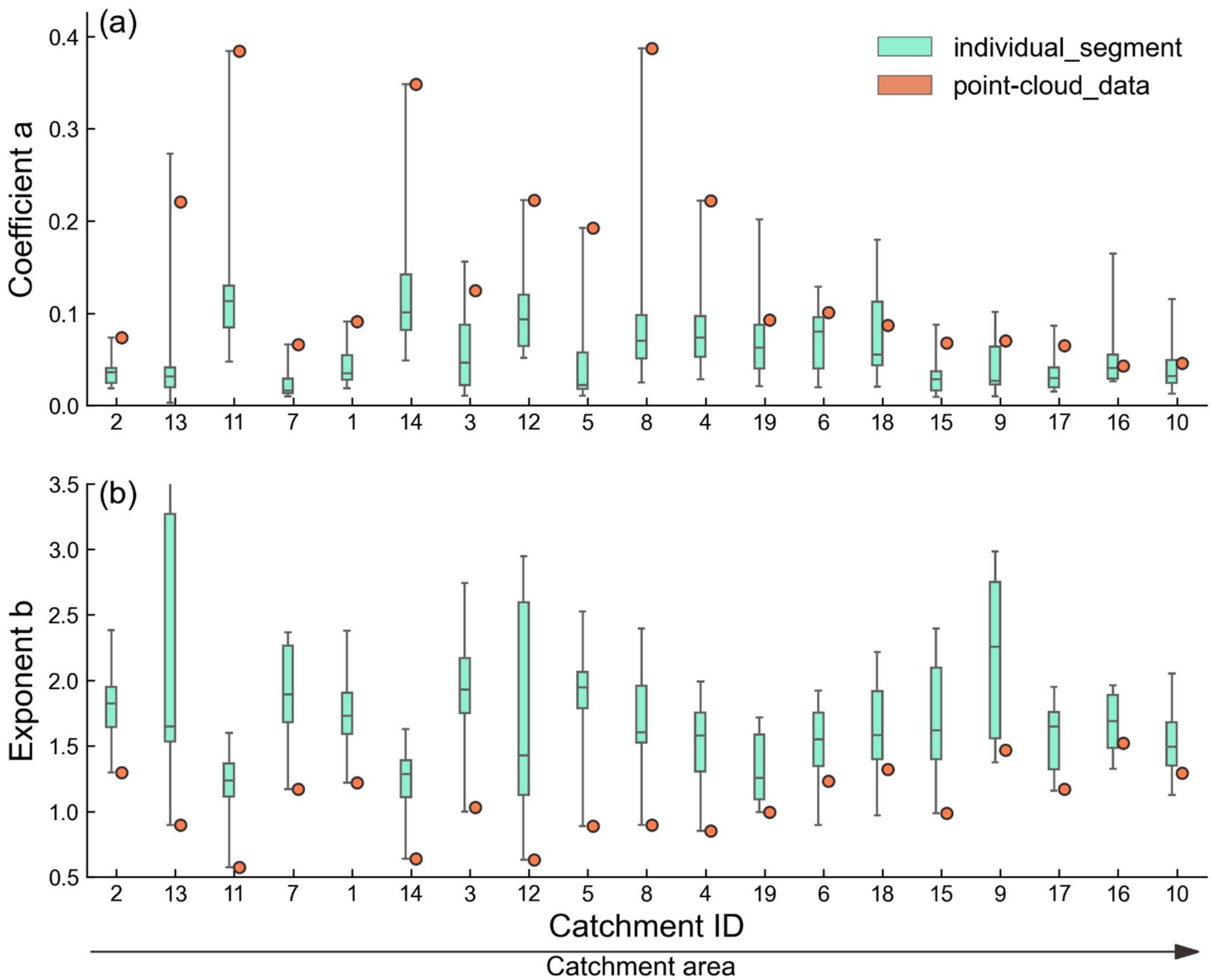

Figure 4: Boxplots of coefficient *a* (a) and exponent *b* (b) derived from the individual recession ~~segment~~segments (cyan box) and point-cloud data (orange dot). The ~~drainage area is used in~~catchments are arranged on the *x*-axis in ascending order~~.~~ according to drainage area. Boxes show the interquartile and data range.

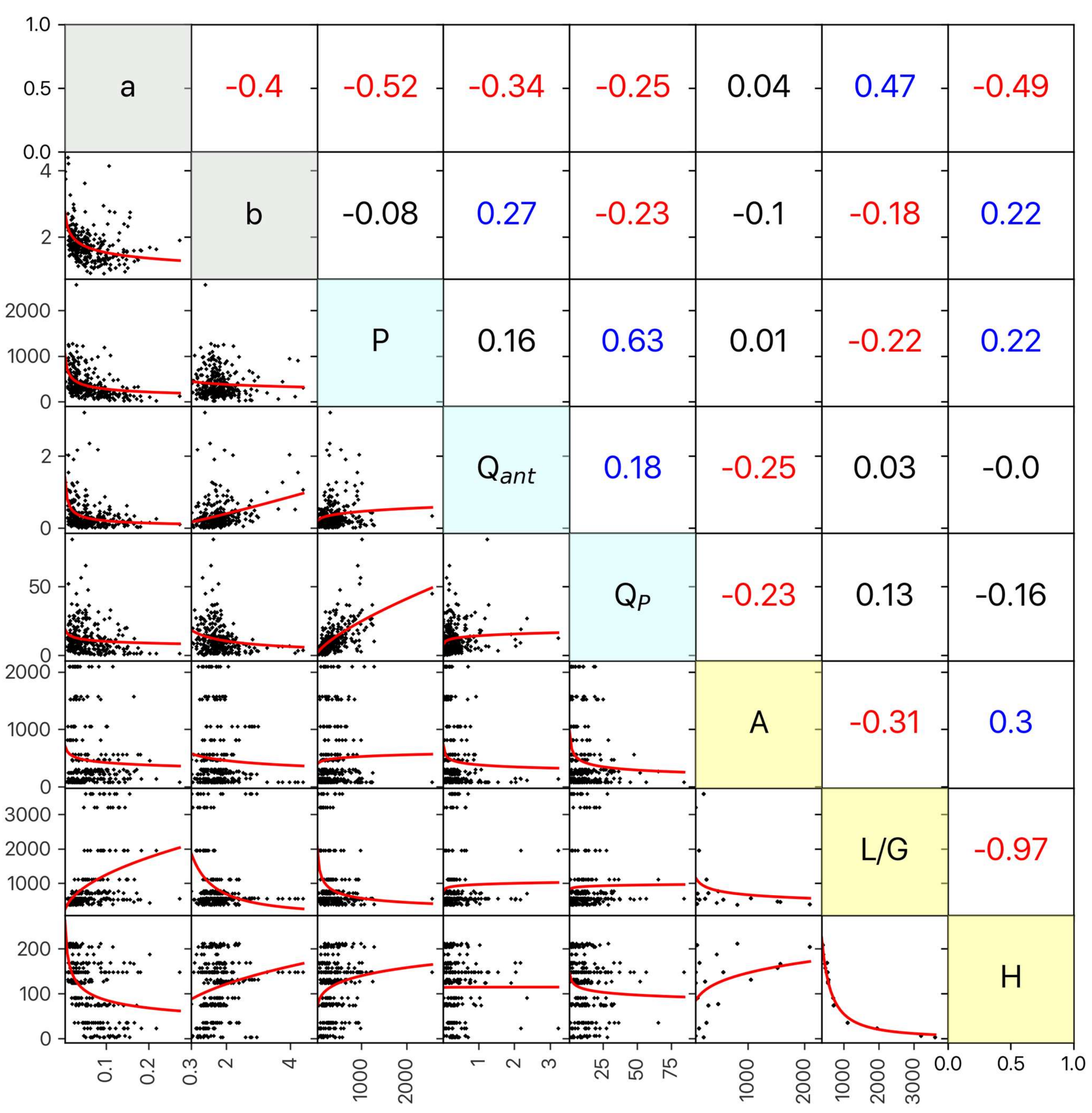
a
b
P
Q_{ant}
Q_P
A
L/G
H
-0.4
-0.52
-0.34
-0.25
0.04
0.47
-0.49
-0.08
0.27
-0.23
-0.1
-0.18
0.22
0.16
0.63
0.01
-0.22
0.22
0.18
-0.25
0.03
-0.0
-0.23
0.13
-0.16
-0.31
0.3
-0.97

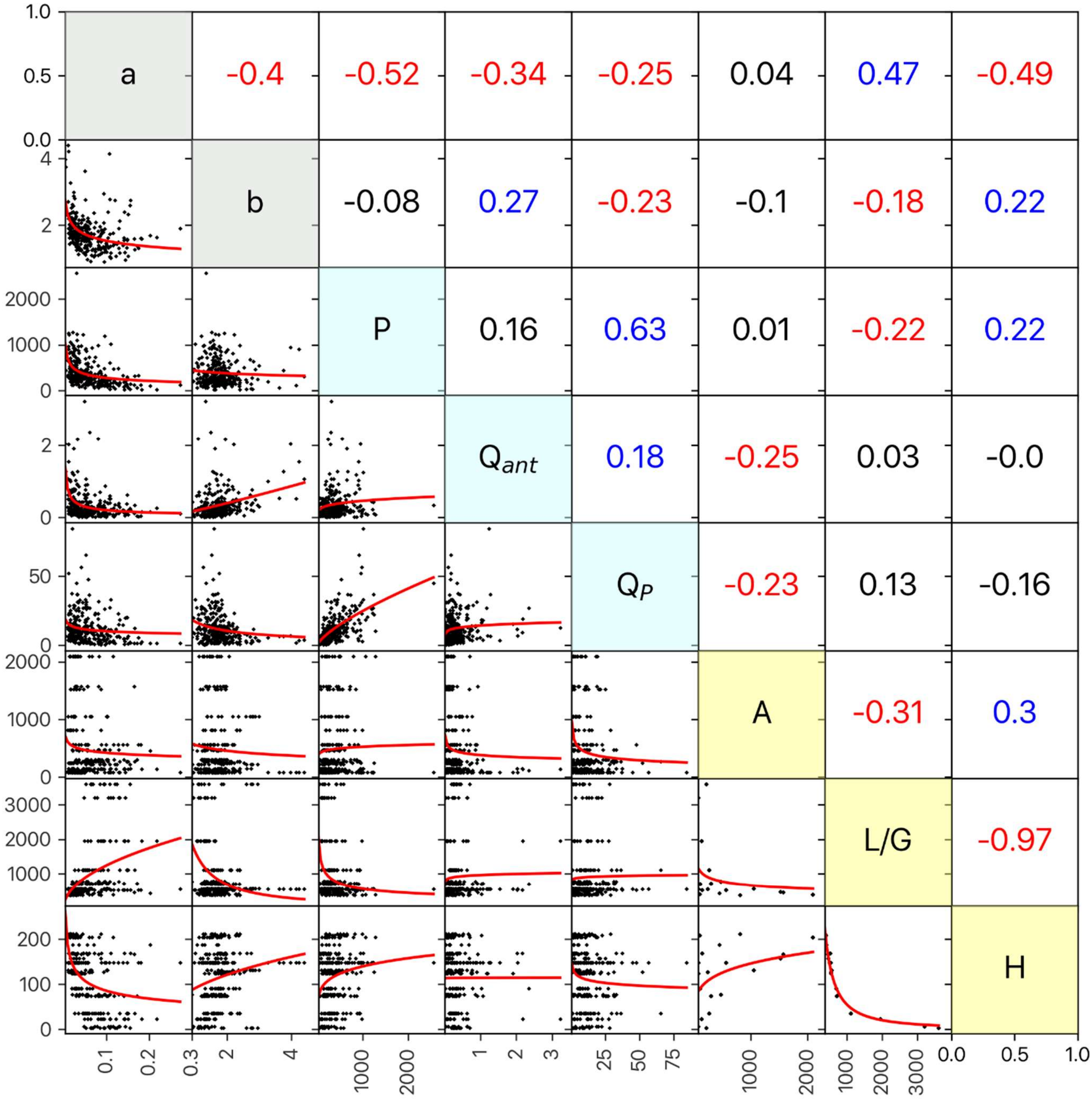

Figure 5: ~~Recession parameter,~~ Correlation of recession parameters *a* and *b* against rainstorm event and landscape variables. Below the diagonal: pairwise scatter plots ~~for~~of the recession parameters and variables with a power-fit regression (red line). Above the diagonal: corresponding Spearman correlation coefficients. ~~Values in blue~~Blue and red ~~color are positive and negative~~ values indicate statistically significant ~~with the 95% level of confidence~~ (p < 0.05~~),~~) positive and negative correlations, respectively. ~~Notes~~Note that all ~~station~~catchments and ~~event~~events are shown in this figure.

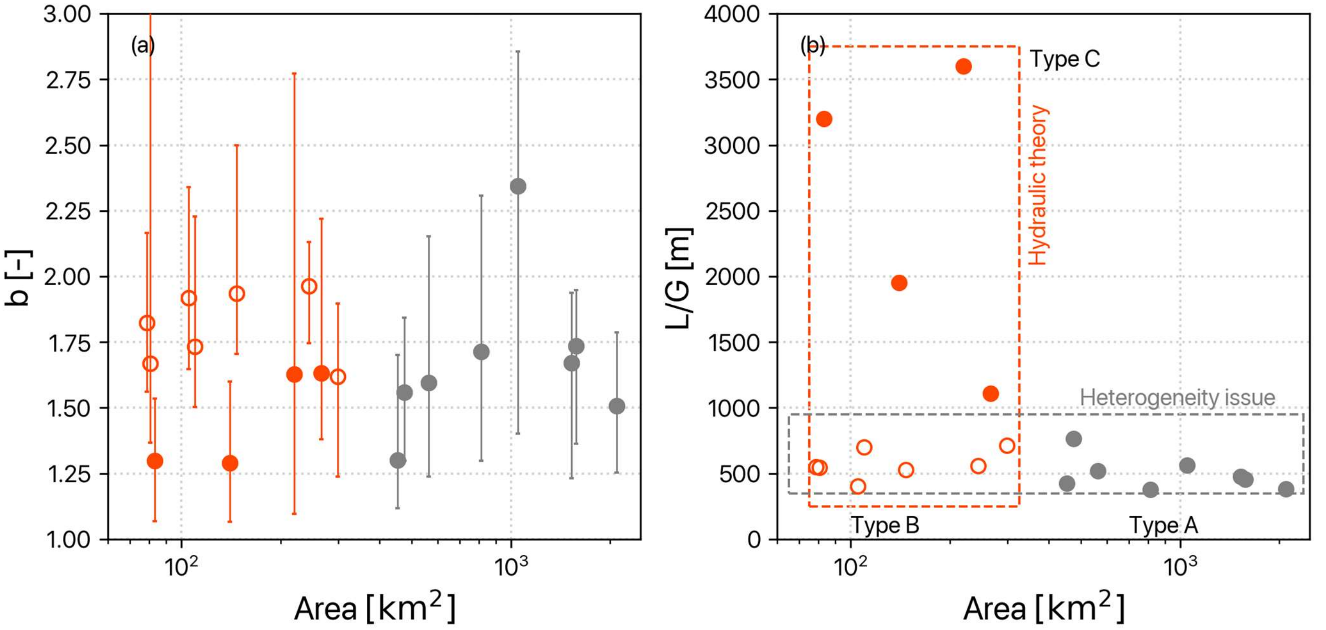

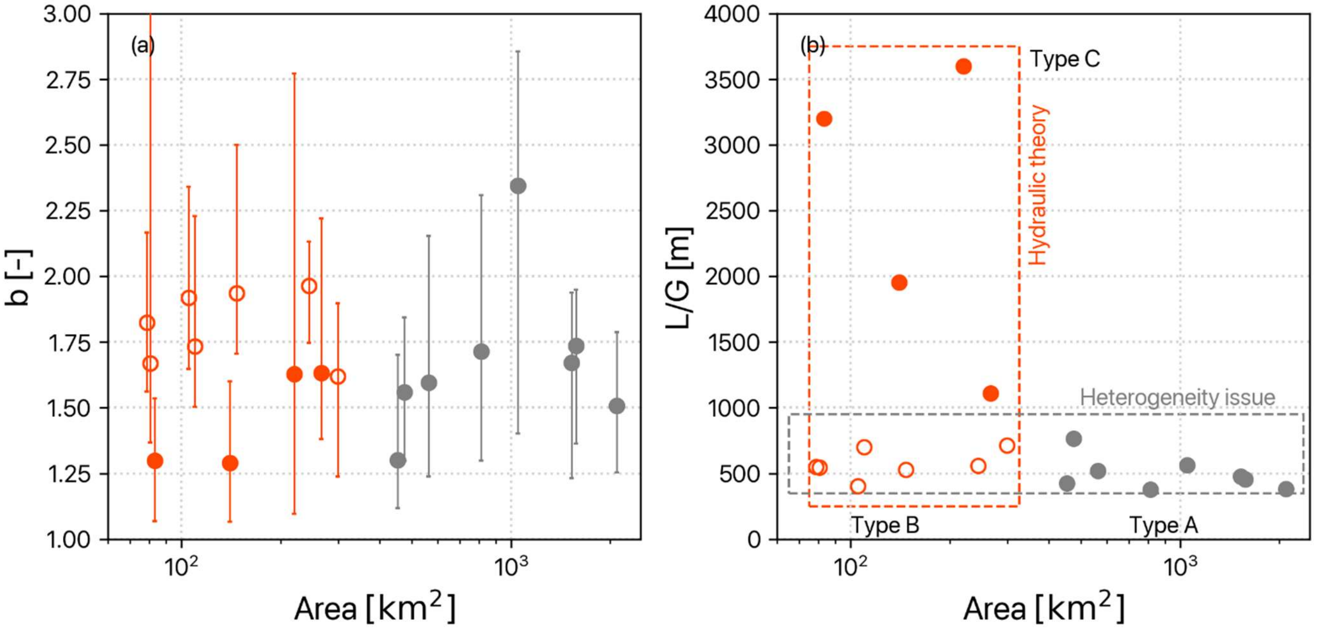

Figure 6: The relationship between drainage area and the recession exponent *b* (a) and the flow path topography (*L*/*G*) (b). The error bar on (a) is the range of the individual segment recession exponent values of each catchment. The orange and gray dots represent small and large catchments (< and > 500 km^2, respectively~~. The~~), respectively, and the solid and hollow dots represent large and small L/G. The recession behaviors in small and large catchments could be explained from two perspectives ~~in terms of~~: hydraulic theory (orange box) and heterogeneity issues (gray box).

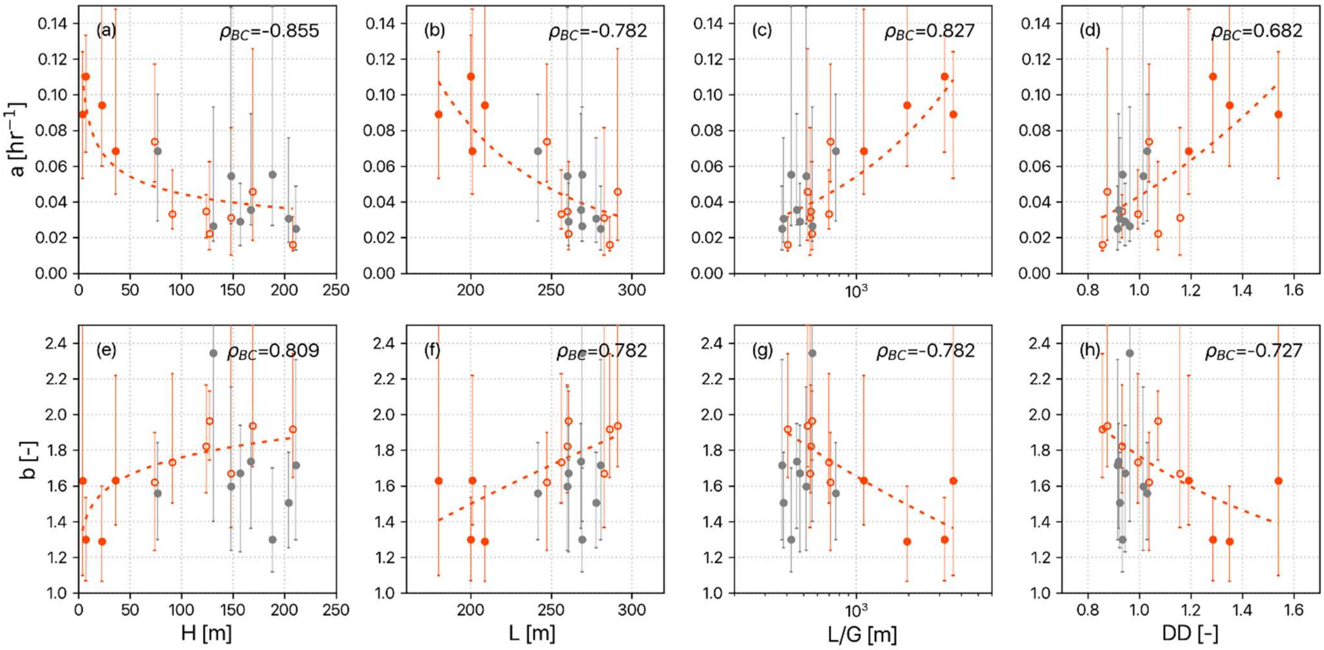

Figure 7: Scatter plots of the median and the range of 10th-90th percentile of recession parameters ~~and~~at each catchment against landscape variables. ~~gray~~Gray solid, orange hollow, and orange solid dots are Type A, B, and C ~~basin~~basins, respectively. The orange dash line is the power-law fit for small catchments (Type B and C~~), respectively.~~). The Spearman correlation coefficient (*ρ*) is listed ~~beside~~in the ~~annotation~~upper-right corner of each panel.

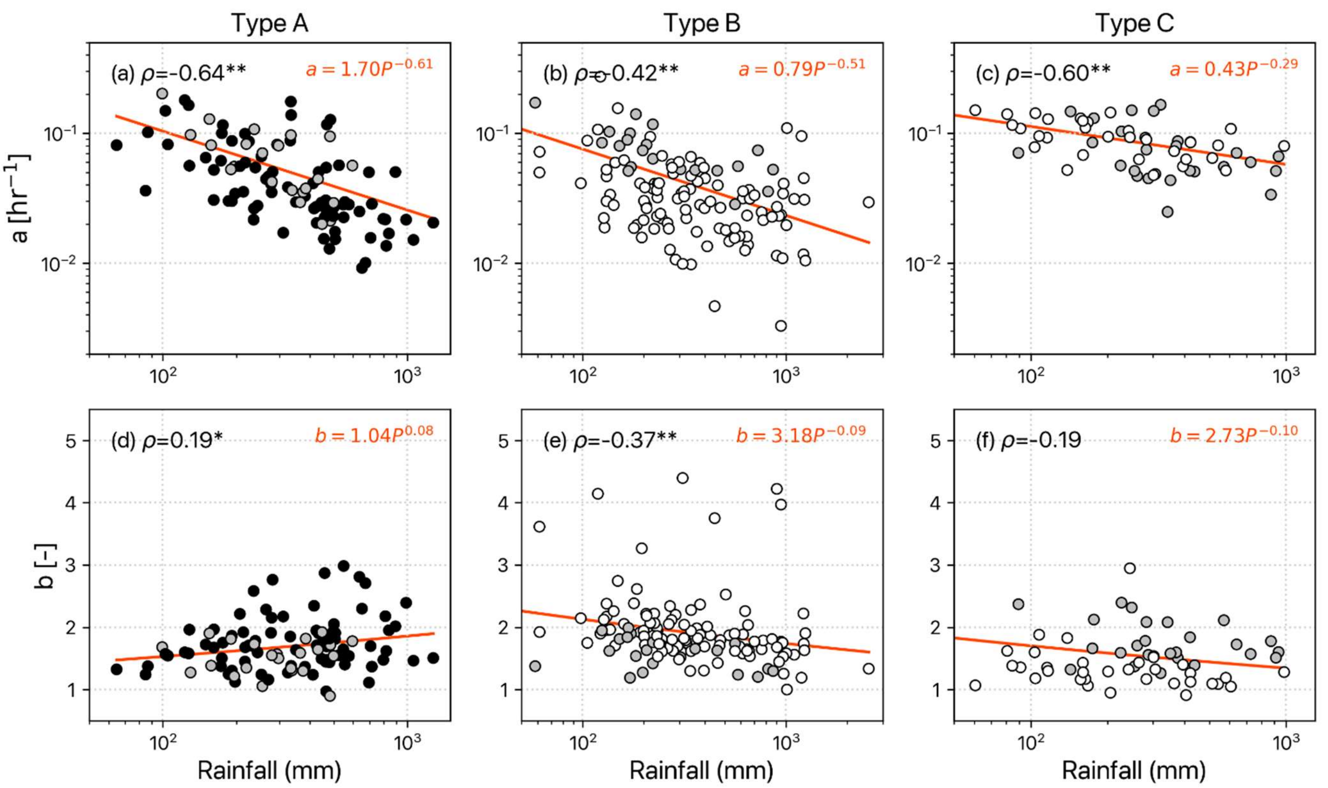

Figure 8: Scatter plots of recession parameters against total rainfall for recession segments at different catchment types~~,~~ ~~corresponding to Fig. 6a.~~. Type A ~~is~~are large catchments (area > 500 km^2), B ~~is~~are small catchments with low *L*/*G* ~~ratio~~ratios, and C ~~is~~are small catchments with high *L*/*G* ~~ratio. The black~~ ratios. Black, gray~~-~~, and white ~~color of dots represents~~dot colors represent the low~~ to~~, medium, and large L/G~~.~~ catchments, respectively. The orange line is the power-law fit curve with ~~spearman~~Spearman correlation coefficients ~~(* and ** means~~ in the upper-left corner of each panel (* and ** denote statistical significance at the 90% and 99% level of confidence, respectively).

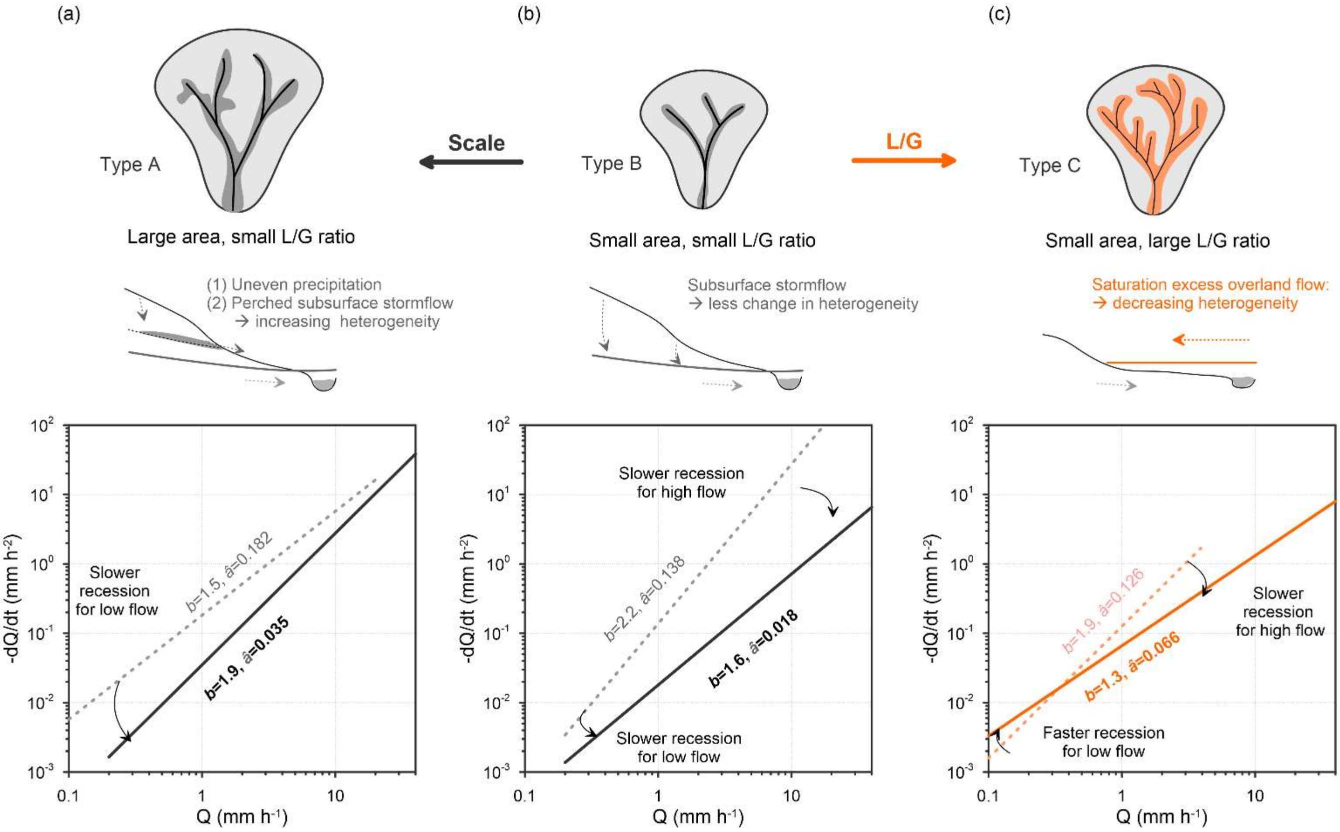

(a)
(b)
(c)
Type A
Scale
Type B
L/G
Type C
Large area, small L/G ratio
Small area, small L/G ratio
Small area, large L/G ratio
(1) Uneven precipitation
(2) Perched subsurface stormflow
→ increasing heterogeneity
Subsurface stormflow
→ less change in heterogeneity
Saturation excess overland flow:
→ decreasing heterogeneity
Slower recession for low flow
b=1.5, â=0.182
b=1.9, â=0.035
Slower recession for high flow
b=2.2, â=0.138
b=1.6, â=0.018
Slower recession for low flow
b=1.9, â=0.126
b=1.3, â=0.066
Slower recession for high flow
Faster recession for low flow
-dQ/dt (mm h-2)
Q (mm h-1)

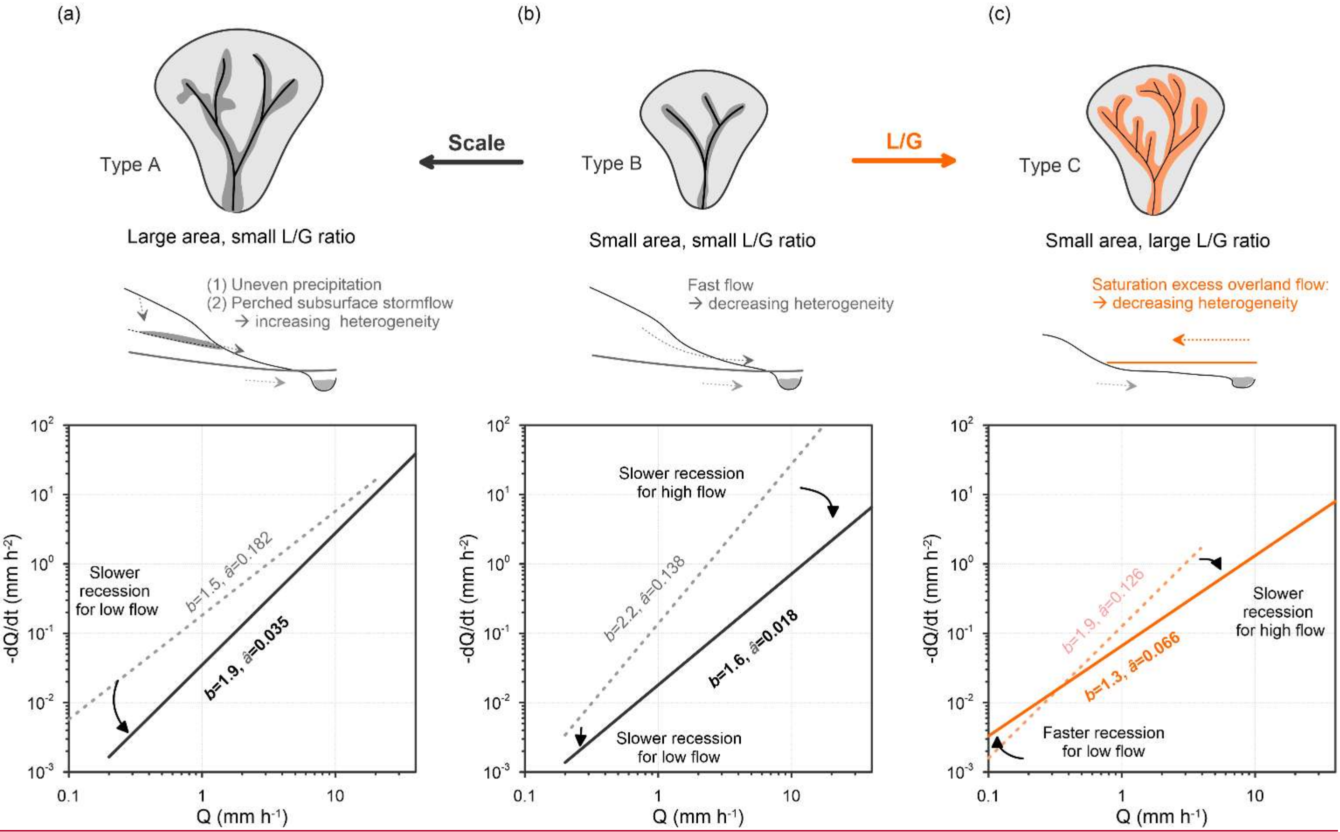

Figure 9: ~~The~~A conceptual diagram ~~demonstrating the regulation of~~illustrating how landscape variables ~~on~~regulate the recession direction ~~of the rainfall-recession relationship.~~during rainstorms. The top ~~panel~~row presents the drainage area and the stream network of three landscape types of ~~catchment~~catchments corresponding to Fig. 6b. The middle ~~panel~~row presents the cross-sectional valley with descriptions of drainage behavior. Here, (a) type A, large catchment and steep slope, drains water via multiple sources of subsurface flow; (b) type B, small catchment and steep slope, drains water via fewer sources of subsurface flow; and (c) type C, small catchment and gentle slope, drains via the extension of the saturated zone along the riparian zone. Correspondingly, the ~~recession~~ bottom row shows how their recession parameters (or regressive line) in recession plots ~~for~~would move from light (dashed line) ~~and~~to heavy (solid line) rainstorms ~~with their recession parameters are presented on the bottom panel~~.